

SCUOLA DI SCIENZE

Dipartimento di Chimica Industriale “Toso Montanari”

Corso di Laurea Magistrale in

Chimica Industriale

Classe LM-71 - Scienze e Tecnologie della Chimica Industriale

I) Improving low photocurrent of
pseudorotaxane based solar cell

II) Synthesis and characterization of new Fe(0)
cyclopentadienone complexes

Tesi di laurea sperimentale

CANDIDATO

Andrea Berneschi

RELATORE

Chiar.mo Prof. Rita Mazzoni

CORRELATORI

Chiar.mo Prof. J.N.K. Joost Reek

Tessel Bowens; Cristiana Cesari;
Anna Gagliardi

Chapter I

Abstract

Next to conventional solar panels that harvest direct sunlight, p-type dye-sensitized solar cells (DSSCs) have been developed, which are able to harvest diffuse sunlight. Due to unwanted charge recombination events p-type DSSCs exhibit low power conversion efficiencies (PCEs). Previous research has shown that dye-redox mediator (RM) interactions can prevent these recombination events, resulting in higher PCEs. It is unknown how the nature of dye-RM interactions affects the PCEs of pseudorotaxane-based solar cells. In this research this correlation is investigated by comparing one macrocycle, the 3-NDI, in combination with the three dyes that contains a recognition sites. 2D-DOSY-NMR experiments have been conducted to evaluate the diffusion constants (LogD) of the three couple. The research project has been stopped due to the coronavirus pandemic. The continuation of this thesis would have been to synthesize a dye on the basis of the data obtained from the diffusion tests and attempt the construction of a solar cell to then evaluate its effectiveness.

Summary

Chapter I.....	3
Abstract	3
1. Introduction.....	6
1.1 Dye sensitized solar cells	6
1.1.1 Harvesting solar energy.....	6
1.1.2 Operational principle of the DSSC.....	7
1.1.3 Improving the efficiency of the p-type DSSC.....	8
1.2 Improving the dye to counteract recombination.....	8
1.3 Dye - redox mediator interactions	9
1.3.1 Dye-Redox mediator interactions in literature	9
1.3.2 Supramolecular interactions	11
1.4 The redox mediator	12
1.5 The pseudorotaxane-based solar cell.....	13
1.5.2 Pseudorotaxane based solar cell	14
1.5.3 The P _N dye.....	14
1.5.4 Redox mediator	15
1.6 Naphthalene diimide as basis for the redox mediator	17
1.7 Aim.....	19
2 Results and Discussion.....	20
2.1 Synthesis of the 3-NDI Ring	20
2.2 Synthesis of bis 2-(2-methoxyethoxy)ethanol-naphtalene and subsequent methylation.....	21
2.3 Interaction between 3-NDI-ring and three different types of Dyes.....	23
2.4 Future research	28
3 Conclusion.....	30
4 Experimental section.....	31
4.1 Synthesis of 2,7-bis(2-hydroxyethyl)benzo[<i>lmn</i>][3,8]phenanthroline-1,3,6,8(2H,7H)-tetraone.	31
4.2 Synthesis of 3-NDI ring	31
4.3 Synthesis of bis 2-(2-methoxyethoxy)ethanol-naphtalene	32
4.4 Methylation of bis 2-(2-methoxyethoxy)ethanol-naphtalene	32
Chapter II.....	35
Abstract	35
1. Introduction	36
1.1 Non innocent ligands.....	36

1.2 Iron Cyclopentadienone complexes	39
1.3 N-Heterocyclic Carbenes	41
1.3.1 Electronic and steric properties	43
1.3.2 The nature of Metal-NHC bond	44
1.4 Catalysis in aqueous environment	46
1.5 Aim of the thesis work	48
2. Results and Discussion	49
2.1 Synthesis of triscarbonyl precursor (Fe ⁰).....	49
2.2 Synthesis of more labile acetonitrile dicarbonyl intermediate (Fe ¹).....	50
2.2 Synthesis of NHC cyclopentadienone complex (Fe ²).....	52
2.3 Synthesis of sulfonated triscarbonyl intermediate (Fe ³)	54
2.4 Synthesis of sulfonated NHC complex (Fe ⁴).....	56
3 Conclusion.....	58
4. Experimental section	59
4.1 Synthesis of (2,4-bis(trimethylsilyl)-7- <i>N</i> -propan-1-ol-bicyclo[3.3.0]hepta-1,4-dien-3-one)iron acetonitrile dicarbonyl (Fe ¹)	60
4.2 Synthesis of (2,4-bis(trimethylsilyl)-7- <i>N</i> -propan-1-ol-bicyclo[3.3.0]hepta-1,4-dien-3-one)iron(1,3-dimethyl-ilidene)dicarbonyl (Fe ²)	61
4.3 Synthesis (A) of ammonium [(2,4-bis(trimethylsilyl)-7- <i>N</i> -propan-1-sulfate-bicyclo[3.3.0]hepta-1,4-dien-3-one)iron triscarbonyl] (Fe ³).....	62
4.4 Synthesis (B) of ammonium [(2,4-bis(trimethylsilyl)-7- <i>N</i> -propan-1-sulfate-bicyclo[3.3.0]hepta-1,4-dien-3-one)iron triscarbonyl] (Fe ³).....	62
4.5 Synthesis of ammonium [(2,4-bis(trimethylsilyl)-7- <i>N</i> -propan sulfate-bicyclo[3.3.0]hepta-1,4-dien-3-one)iron(1,3-dimethyl-ilidene) dicarbonyl] (Fe ³)	63
5 Reference.....	64
Chapter I.....	64
Chapter II.....	66

I. Introduction

1.1 Dye sensitized solar cells

1.1.1 Harvesting solar energy

Nowadays, most energy is still generated by burning fossil fuels such as petroleum and coal. However, burning fossil fuels raises the CO₂ levels in the atmosphere, causing global warming. Therefore, the world needs to transition towards a sustainable source of energy. Solar power is the answer to this problem, as the Sun provides enough power for current and future demand. The Earth receives almost 5000 times as much energy from the sun as currently is being used by humans in a year.¹ Using a solar panel, this energy can be converted directly into electrical power.² Furthermore, photoelectrochemical cells can be used to convert energy into fuel.¹

Developing solar panels that are both efficient and cheap is an important goal in aiding the transition towards the use of solar power. As of 2020, silicon solar panels are conventionally used. Their power conversion efficiency (PCE, electrical power generated per amount of solar power provided) is high, with records held of above 25%.³ However, they require high manufacturing costs and the cells itself are inflexible and typically heavy.⁴ Dye sensitized solar cells (DSSC) could be an additional way to provide solar energy, as they use cheap materials and provide ease of manufacturing in mass-production scale.⁵ DSSC, belonging to the group of thin-film solar cells, are lightweight and flexible, in contrast to silicon solar panels. Furthermore, they can work efficiently, under diffuse light and could therefore be used in indoor applications.⁶ This opens new areas of possible applications. such as building integrated photovoltaics (BIPV), where solar panels are built into, for example, roofs, walls or windows. Research towards improving the efficiency of DSSC has been of great interest, as this efficiency is still lower than the conventionally used silicon solar panels.⁷ With the knowledge of DSSC, we can design and construct photoelectrochemical cells. In photoelectrochemical cells, the absorbed solar energy is directly used to facilitate a reaction like the reduction of CO or the electrolyzation of water into hydrogen and oxygen gas. The hydrogen can then be used as a fuel.¹ This way, the generated energy can be stored and used in circumstances with less sunshine. This research concentrates on DSSCs and aims to improve these, focusing on the interaction between two of its components: the dye and the redox mediator. An introduction on these terms is given below.

1.1.2 Operational principle of the DSSC

A DSSC (**Figure 1**) is composed of a molecular dye covering a semiconductor layer. The electrons of the dye can absorb sunlight and thereby get excited. This causes them to move towards the counter electrode, often made of platinum. All of this is immersed in a liquid conductor, the electrolyte. Redox mediator molecules of the electrolyte transport electrons between the dye and the counter electrode. There are two types of DSSC, n-type and p-type. P-type DSSC mainly use NiO, while n-type mainly use TiO₂.

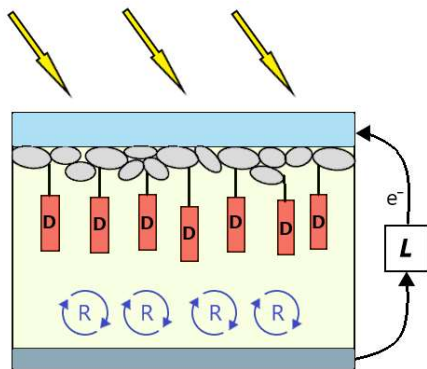


Figure 1 General design of a dye sensitized solar cell

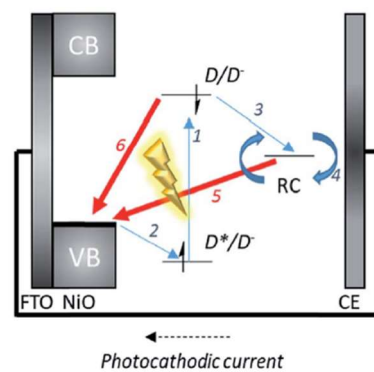


Figure 2 Operation principle of a p-type DSSC³⁴

In n-type DSSC the excited electron is injected into the conduction band of the semiconductor. This results in the oxidation of the sensitizer. The electrons then move via the back contact to the counter electrode. A redox mediator in the electrolyte reduces the sensitizer again. The oxidized mediator diffuses towards the counter electrode and is reduced there, closing the circuit.⁸ Complementary to n-type, in p-type cells an electron is transferred from the valence band of the semiconductor to the dye (1) (**Figure 2**), where it is excited (2). Then it is transferred to the redox mediator (3), creating a charge separated state. The sensitizer is reduced by the semiconductor (4). The electron in the redox mediator can recombine with electron holes in the dye (5) or the valence band (6).⁹ Recombination is an undesirable process that does not yield any current and needs to be dealt with to improve PCEs.

1.1.3 Improving the efficiency of the p-type DSSC

In theory, p-type cells should be able to operate as efficiently as n-type cells, but in practice this is not yet realized. This is mainly because of the recombination of the electrons with electron holes. Research towards DSSC is mainly concerned with n-type cells,¹⁰ which cannot provide solution for the recombination problem in p-type cells.¹¹ Current record-efficiencies are 15% for n-type DSSC¹² and 2.51% for p-type DSSC.¹³

Improving the efficiency of p-type cells eventually allows for the development of dye sensitized tandem cells, with a p-DSSC as the cathode and an n-DSSC as the anode. These cells have a theoretical efficiency that is higher than the theoretical limitation for single p- or n-type cells. A single solar cell has a theoretical efficiency limit of 33.7%; the Shockley-Queisser limit.¹⁴ This means that without recombination, only 33.7% of the solar energy reaching the solar cell surface can be converted into electrical energy. The main reason for this is that it is physically impossible for the dye (in the case of a DSSC) to absorb the full spectrum of the sunlight, making energy loss inevitable. Photons with an energy that is less than the gap between the ground state and the excited state of the dye will not be able to excite electrons and contribute to generating electricity. Meanwhile, the excess energy of photons with an energy that is higher than that of the gap will not be utilized.

The theoretical limit can be raised to 42% by creating a tandem structure of two cells,¹⁵ because then electrons are excited in two different materials and a broader part of the spectrum can be utilized.¹⁶ However, one of the main reasons that this efficiency is not yet approached is because a tandem cell is limited by the electrode with the smaller photocurrent. This is the p-DSSC because of its sub-optimal performance.¹⁷

1.2 Improving the dye to counteract recombination

One of the proposed answers to prevent recombination p-type DSSC is the design and use of a push-pull dye. In a push-pull dye, the highest occupied molecular orbit (HOMO) of the dye lies close to the NiO, and the lowest unoccupied molecular orbit (LUMO) lies far away from this surface. This counteracts the recombination pathway of the excited dye back to the semiconductor.¹⁸ Bach and co-workers proposed the PDI dye in **Figure 3**, in which a linker moiety is introduced to increase the distance of the LUMO of the dye to the semiconductor surface.¹⁹

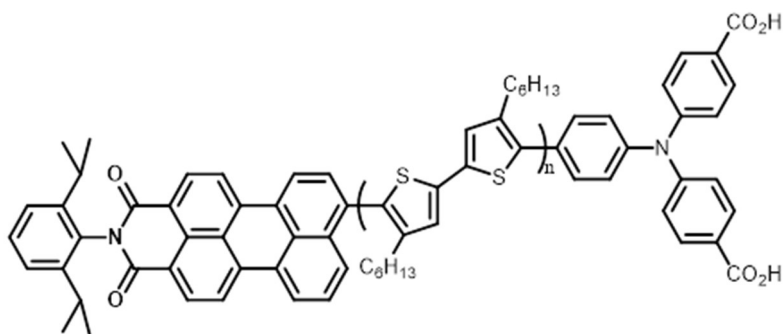


Figure 3 PDI dye as proposed by Bach and co-workers²⁰

This increased the charge separated state, which caused a decrease in recombination rate by five orders of magnitude. Although this is an impressive improvement, it was found that there was little driving force to transfer the electron from the reduced dye to the redox mediator when the iodine couple was used. When a cobalt based redox mediator was used instead, the PCE was improved from 0.41% to 1.3%.¹⁸ With an iron based redox couple, this dye was used to set the current PCE record for p-type cells to 2.51%.¹³

1.3 Dye - redox mediator interactions

Most research in preventing recombination from happening in DSSC is concerned with one component of the system, such as the dyes described above. However, even though the PDI dye did prevent recombination, its true worth was not shown until the correct redox mediator was used.

Improving one component of the system is indispensable in reaching higher efficiencies, but looking at the system as a whole, designing its parts to collaborate might lead to new angles of approach to improve the efficiencies of DSSC even more. A promising example of this is exploring interactions between the dye and the redox mediator.

1.3.1 Dye-Redox mediator interactions in literature

One of the main problems causing recombination in p-type OSSC is the relatively slow speed of the electron transfer from the dye to the redox mediator. The Marcus theory states that the speed of electron transfer depends on a combination of two factors: the energy difference of the relevant orbitals of the two systems and their physical distance.²⁰⁻²¹

If the energy difference is too small, there is no driving force for the electron to transfer. However, if the energy difference is too big, there is no sufficient overlap of the orbitals, lowering the rate of electron transfer. The lower the physical distance, the better the orbital overlap and the higher the electron transfer speed.

In regular DSSC, the distance between the redox mediator and the dye is dictated by diffusion of the redox mediator in solution. Zahn and co-workers²² investigated dye-redox mediator interactions in p-type devices, to promote the coordination of the redox mediator to the dye, increasing the speed of the electron transfer. Diverse Cu, Ni and Co redox mediators were computationally screened on the orbital overlap between these complexes and the dye. Of the best performing couple, Co(II)TPP and the Py₃N dye (**Figure 4**), a solar cell was constructed.

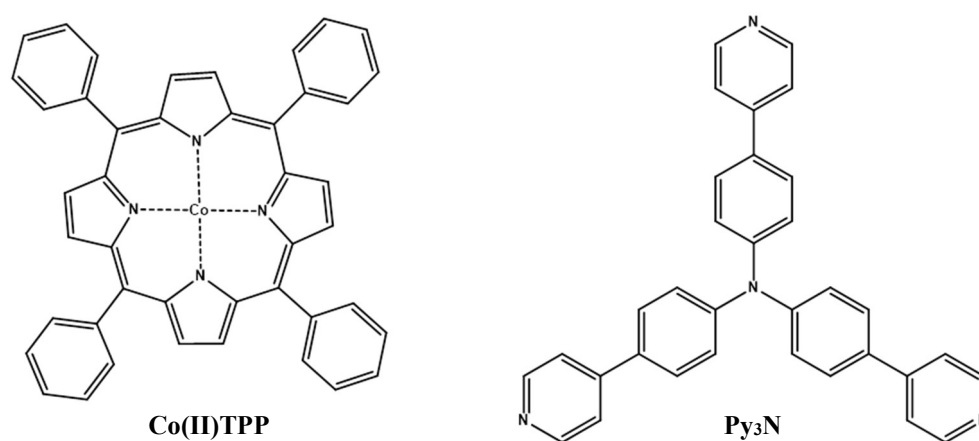


Figure 4 Redox mediator and dye as used in solar cell by Zahn and co-workers²²

The system employed dipole-dipole interactions, meaning that electron poor redox mediators did have an affinity for the dye and, when they were reduced and became electron rich, repelled the dye.

Unfortunately, their constructed solar cells did not yield higher efficiencies than analogous cells with the iodine couple as redox mediator. They conclude the limiting factor is in the speed of the electron transfer of the semiconductor to the dye. Furthermore, they suggest that the beneficial effects of the dye-mediator interactions can be observed if a push-pull dye is employed, because such a dye increases the speed of electron transfer from the semiconductor to the dye. Berlinguette was the first to design a system that it can support preorganization of the redox mediator on the dye. This increases the chance of a redox mediator being close to the dye when it is excited, increasing the speed of the electron transfer.

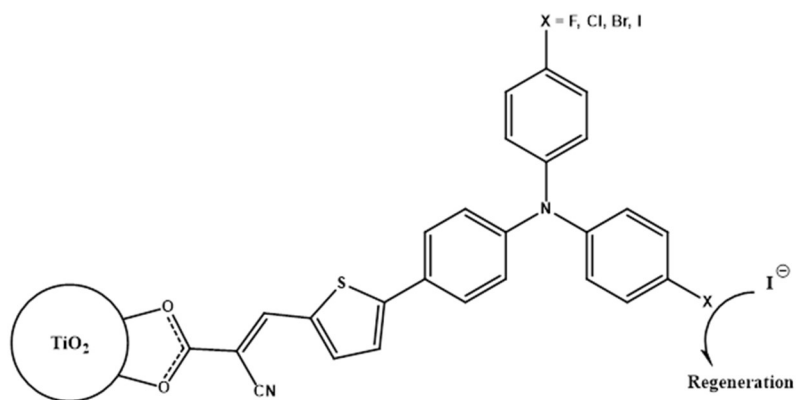


Figure 5 Dye-Redox mediator interaction of Berlinguette²³

Berlinguette's system used the iodine couple as a redox mediator but added halogens to the dye to utilize halogen bonding as a means for preorganization (**Figure 5**). This system design led to a great increase in electron transfer speed, measured by looking at the regeneration of electrons on the dye. The efficiency of the system also increased.²³ The iodine couple is not ideal in terms of reduction potential for p-type DSSC. For these systems, a new dye and redox mediator should be designed together. However, the result implies that weak intermolecular interactions between dyes and redox mediators can improve the solar cell efficiency.

1.3.2 Supramolecular interactions

Interactions between the dye and the redox mediator should utilize weak interactions, as the mediator should still be able to move away from the dye after electron transfer has occurred. Covalent bonds are too strong to be reversible in this context. Supramolecular bonds, non-covalent bonds between molecules, should be employed. These kinds of interactions include for example van der Waals interaction, hydrogen bonding and dipole-dipole interactions. Other interesting intramolecular behavior, also known as π - π interactions,²⁴ are the attractive, noncovalent interactions between aromatic rings. Although the precise nature of these interactions is under debate,²⁵ it is shown that π -systems can stack to form sandwich complexes. These complexes are more favorable if one of the π -systems is electron rich and the other electron poor. Otherwise, the two π -systems will repel each other, reducing the stacking interaction.²⁴ Utilizing these interactions could be an interesting option for dye-redox mediator interactions, as changing between electron poor and electron rich is in the very nature of the redox mediator.

1.4 The redox mediator

The type of redox mediator used is a great contributing factor in the performance of the DSSC.²⁶ This is because of their influence on both the charge recombination and the Voltage at Open Circuit (V_{OC} , the maximum voltage at zero current). Charge recombination is one of the main performance-limiting factors of p-type DSSC.²⁷ It is believed that a lack of charge separation increases the chance recombination happens.²⁸

In p-type DSSC, the iodine couple has been used since the beginning of DSSC development as a redox mediator, and still yields one of the most efficient and stable DSSC.²⁹ However, the iodine couple has a reduction potential of 0.40 V and the commonly used P1 dye -0.87 V.²⁷ The more positive a reduction potential of a species is, the greater its affinity for electrons.

This energy difference of 1.27 V, as the iodine couple and the dye in the p-type system have, is so large that it is hampering the speed of electron transfer to the iodine couple, as stated by the Marcus theory. Exciting the electron in the dye is a very fast process, in the order of picoseconds, and the electron transfer to the iodine couple is slow, occurring on microsecond scale.³⁰ Electron recombination also occurs on microsecond scale.³⁰ This means that an electron has high chances of recombining instead of contributing to the current, leading to suboptimal performing solar cells.

The reduction potential of the iodine couple also limits the V_{OC} of the DSSC. The maximum voltage of a DSSC is determined by the energy difference of the valence band of the semiconductor and the highest occupied molecular orbit (HOMO) of the reduced redox mediator; the effective energy difference between the electron in its 'resting state' and the excited electron at the moment it is delivered to the counter electrode. The difference in energy between the excited dye and the reduced redox mediator is lost in the form of heat; another reason it is important that this energy difference is minimal.

Improving the redox mediator - dye combination to increase the speed of the electron transfer is essential in improving the efficiency in DSSC.

1.5 The pseudorotaxane-based solar cell

The pseudorotaxane based solar cell (PR-SC) is a proposed answer to the charge separation problem of p-type DSSC, employing dye-redox mediator interactions to reduce recombination.

1.5.1 Pseudorotaxanes

Rotaxanes are a type of molecular architecture in which a macrocyclic molecule is formed around a molecular thread, which has bulky moieties on each end. The internal diameter of the macrocycle is smaller than these bulky molecules, preventing the macrocycle from unthreading. A pseudorotaxane is similar to this, except that one of the thread ends does not contain a bulky molecule and the macrocycle is able to leave the thread.³¹

Pseudorotaxanes are used to construct various types of molecular machines.³² The combination of a paraquat ring and naphthalene recognition site on the thread is often used in pseudorotaxane based molecular devices. An example (**Figure 6**) is a molecular switch as documented by Stoddart and co-workers, the group to introduce these types of molecular constructions.³³ Upon addition of alkali metal cations, the paraquat ring is being repulsed from the naphthalene thread. This switch can be observed from a change in the absorption spectrum, which makes them optically responsive.

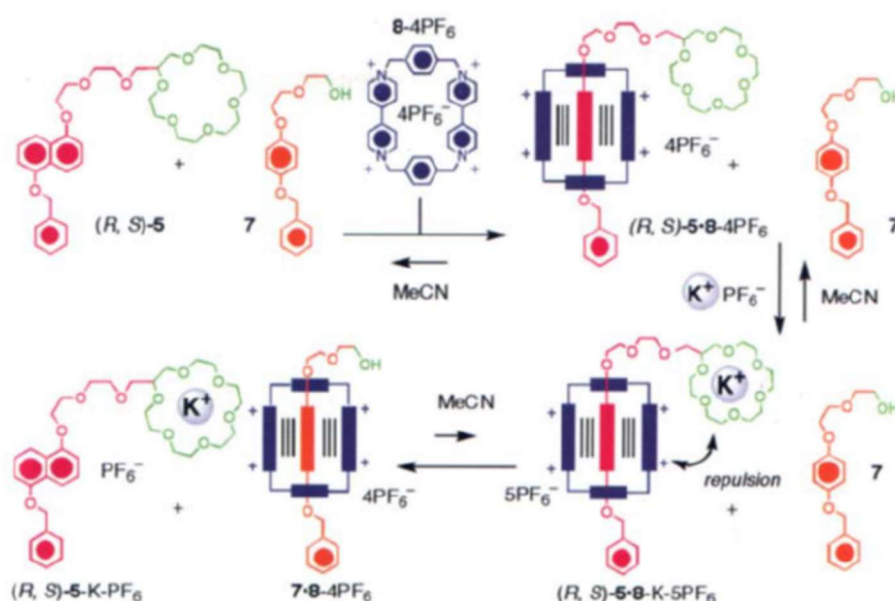


Figure 6 Molecular switch based on pseudorotaxanes³³

1.5.2 Pseudorotaxane based solar cell

One way to achieve a charge separated state is by physically separate the mediator from the dye after electron transfer. This system is schematically described in **Figure 7**. Here, an organic macrocycle is used as the redox mediator. It can coordinate via π - π interactions to a recognition site bound covalently to the dye. The π -system of the ring is electron deficient, while the recognition site is electron rich. If the ring is reduced by the dye, it now being electron rich makes it lose its affinity for the dye. As it moves away, creating a charge separated state. At the counter electrode, the reduced ring is oxidized again. Oxidized rings that have diffused back to the recognition site on the dye will take the place of the reduced ring, closing the circuit. This system was previously described for the first time by this group.³⁴

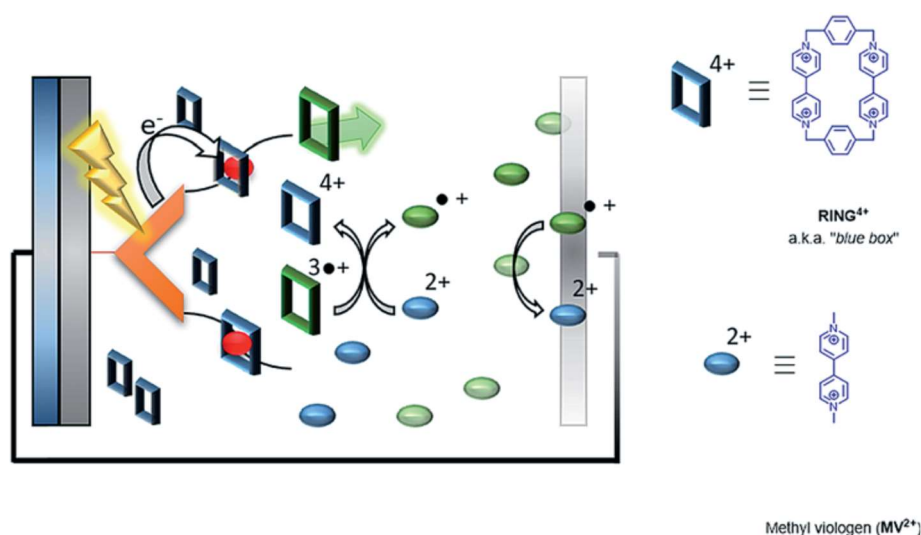


Figure 7 Principle of the PR-SC³⁴

1.5.3 The P_N dye

The design of the dye was based on the **P1** dye as depicted in **Figure 8**, which was first reported in 2008 by the group of Sun.⁸ The **P1** dye uses a triphenylamine moiety as the electron donor, a malononitrile moiety as the electron acceptor, and a thiophene unit as the conjugated chain connecting them. The dye is attached to NiO, the semiconductor of the solar cell, using the carboxylic acid group. This design causes it to behave as a push-pull dye (**Figure 10**). This lowers the chances of an excited electron in the dye to move back to the NiO surface. With this dye, iodine-based solar cells were constructed, giving efficiencies of 0.12%.³⁵

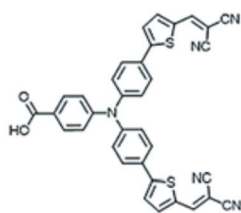


Figure 8 The **P1** dye³⁴

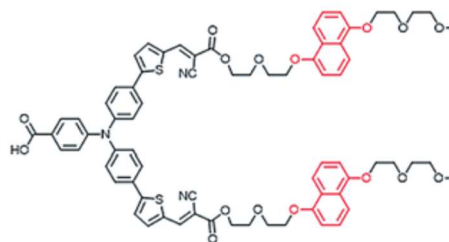


Figure 9 The **PN** dye³⁴

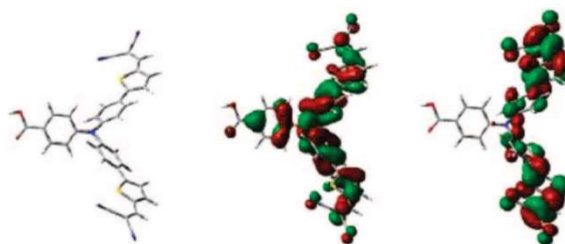


Figure 10 HOMO (middle) and LUMO (right) of the **P1** dye³⁴

The **PN** dye is similar to the **P1** dye but has a naphthalene moiety with polyethylene glycol (PEG) side-chains connected to the malononitrile moiety (See **Figure 9**). This naphthalene moiety is an electron rich aromatic system, allowing for electron deficient aromatic systems to coordinate to it via π - π interactions. It functions as the thread in a pseudorotaxane, with the redox mediator being the macrocycle **Ring 1** (**Figure 11**). It was found that the **PN** dye is very similar way to the **P1** dye in terms of performance for the commonly used iodine couple.³⁴ The absorption spectra both have peaks at 345 and 468 nm, with the **PN** dye having extra peaks between 270 and 340 nm arising from the linker moieties. Furthermore, **PN** was found to have a reduction potential at 0.9 V, which is very close to that of the **P1** dye at 0.88 V.

1.5.4 Redox mediator

A paraquat ring was used as the redox mediator (**Figure 11**). The results show a clear difference in behavior between the paraquat ring and paraquat itself, the non-cyclic starting compound for making this ring. The latter gives the same results regardless of whether **PN** or **P1** is used. A clear increase in performance in terms of current is observed when **Ring 1** is added to the solar cell.

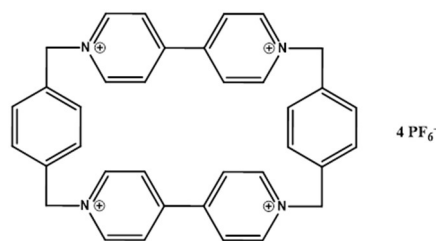


Figure 11 Ring1³⁴

This effect is only seen for the **P_N** dye and not the **P_I** dye. This indicates that there is indeed a beneficial interaction occurring between the ring and the coordination site of the dye (**Table 1**, **Figure 12**). The maximum voltage and efficiency could only be measured for cell 4 and were 0.0003% and 0.179 V, respectively.

Cell	Dye	Redox couple	J _{sc} (μA·cm ⁻²)
1	P_I	Paraquat only	-1.31
2	P_I	0.3% Ring1 + Paraquat	-1.02
3	P_N	Paraquat only	-1.41
4	P_N	0.3% Ring1 + Paraquat	-9.56

Table 1 Obtained J_{SC} values for the four different constructed DSSC³⁴

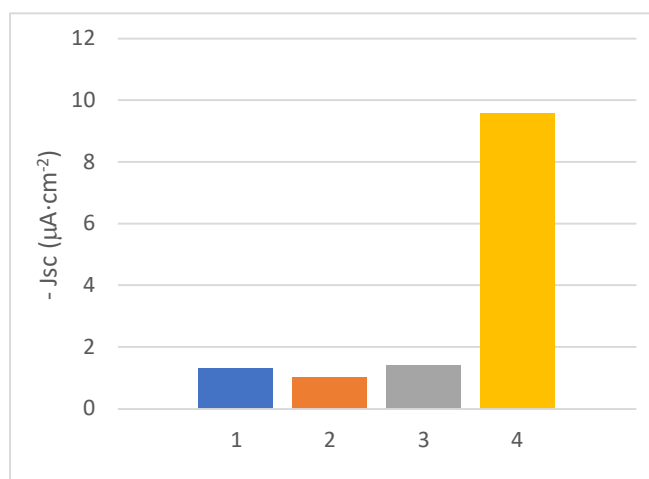


Figure 12 Bar chart of J_{SC} in **Table 1**³⁴

However, the absolute current of the **P_N** - **Ring 1** combination is still significantly lower than when the iodine couple is used as a redox mediator, which gives J_{SC} values in the order of few mA · cm⁻².²⁷ Therefore, this research serves as a proof of principle of the PR-SC and opens up an opportunity to improve this system.

There are several aspects of the design that can be improved. One of the most important ones is hypothesized to be the relatively strong binding constant between the ring and the coordination site of the P_N dye ($K_{\text{ass}} : 3.4 \times 10^4 \text{ M}^{-1}$). If this interaction is too strong, the diffusion of the ring away from the dye could be slow as a consequence. This would decrease the efficiency of the redox mediator, as the diffusion towards the counter electrode will also be slow.

A reason for this strong binding constant might be the quadruple positive charge of the ring. As the coordination site is electron rich, it will have a powerful interaction with the ring. This interaction will be strong even after it has taken up an electron, as it still has a charge of 3+.

Another point of improvement is the reduction potential of the ring. This lies at -0.10 V, which is a substantial difference with the dye at -0.90 V.³⁴ A large potential difference leads to a slow electron transfer, increasing the chances of recombination. Furthermore, it lowers the maximum voltage that can be reached with the system, as that is dictated by the difference between the reduction potential of the semiconductor and that of the redox mediator.

1.6 Naphthalene diimide as basis for the redox mediator

A redox mediator of the PR-SC needs to be a molecule that can undergo reversible electrochemistry, to be able to transport electrons, and it is required to have some sort of interaction with the recognition site on the dye.

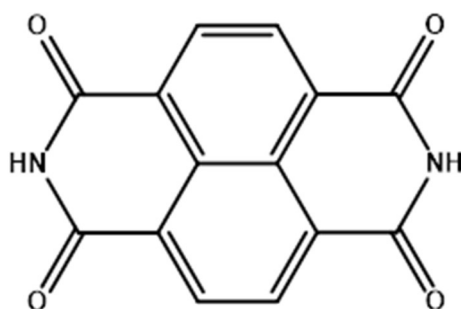


Figure 13 1,4,5,8-naphthalene diimide

The design of the redox mediator will be based on 1,4,5,8-naphthalene diimide (NDI) (**Figure 13**). These molecules are planar, chemically robust and redox active.³⁶ These properties are desirable for the ring, as the reduction should be reversible in the context of a solar cell, in which a great variety of molecules is present.

Naphthalene diimides are a class of electron deficient aromatic compounds, while the aromatic system of the recognition site on the dye is electron rich. Therefore, the NDI is expected to be able to coordinate to the existing recognition site of the dye using π - π interactions. When it gets reduced by one electron, the now electron rich aromatic system will repulse the dye, likely causing the NDI to move away from it. This is the interaction that is desired for this design. Furthermore, Hansen and co-workers showed a case of C-H--O hydrogen-bonding interactions between the diimide methylene hydrogen and the central oxygen atom of a crown polyether chain.³⁷ This interaction could also aid the coordination of an NDI to the recognition site.

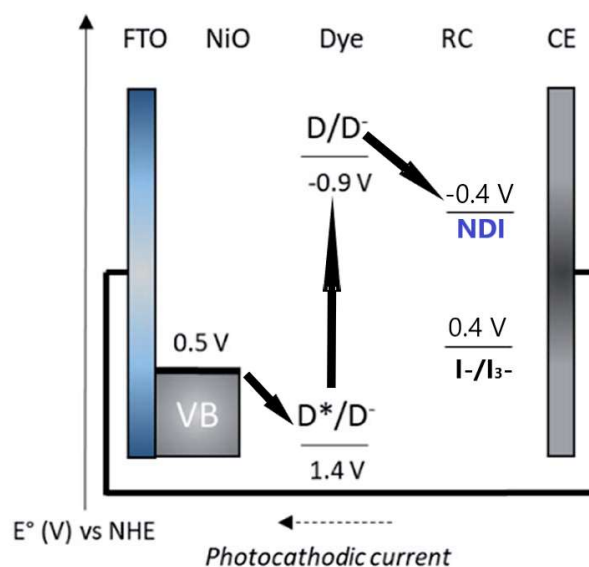


Figure 14 Schematic overview of reduction potential of several parts of the solar cell³⁴

Research shows that naphthalene diimides can undergo single reversible one-electron reduction. The potential for NDI itself is -0.38 V in DCM.³⁶ This value is promising, as it lies between the potential of the used dye (-0.90 V) and that of the semiconductor NIO (0.50 V).³⁸ A redox mediator in a p-type cell must be able to undergo reduction by the dye and able to regenerate the redox mediator. To achieve this, its reduction potential needs to be in between that of the dye and the electrode.¹⁰ Furthermore, this reduction potential is closer to the dye than the reduction potential of the commonly used iodine couple (0.40 V), leading to a higher power efficiency and faster electron transfer. In **Figure 14**, the relevant reduction potentials are depicted schematically.

These characteristics seem to be promising for improving the performance of the PR-SC, when a redox mediator is designed based on NDI. Since NDI is not positively charged, it might have

a lower binding constant with the recognition site of the dye. Additionally, the molecule becomes negatively charged when reduced (instead of going from 4+ to 3+ for Ring 1). This might increase the repulsion movement from the recognition site.

According to this statement 3-NDI ring (**Figure 15**) was developed by my research group as the redox mediator.

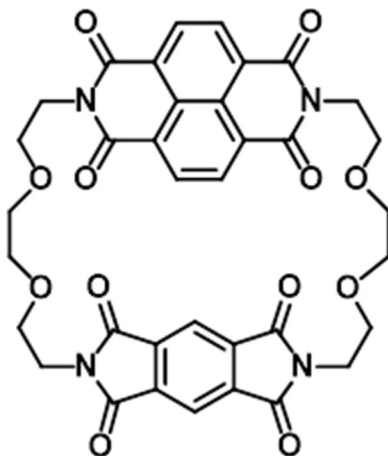


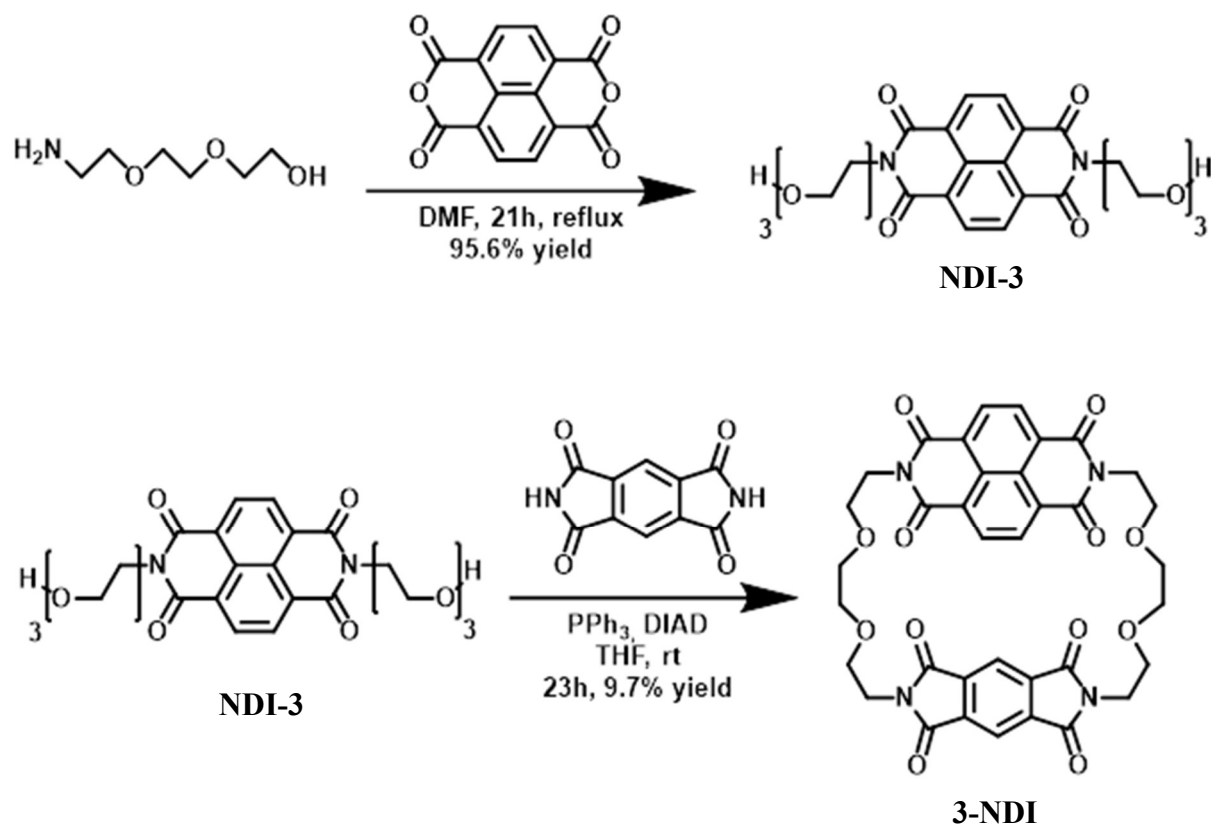
Figure 15 3-NDI ring

1.7 Aim

The low photocurrents of the previously described PR-SC could possibly be improved by designing a new system with a lower binding constant between the dye and the redox mediator. This can be achieved by either changing the dye and its interaction site or by changing the redox mediator. To provide for a clear comparison to the previous design of the PR-SC, the dye and the redox mediator should not be changed at the same time. The aim of my research project was to improve the dye, using the 3-NDI Ring as a redox mediator. The interaction between three different dyes and the redox mediator was evaluated. In particular, trying to exploit the use of a push-pull dye to limit recombination.

2 Results and Discussion

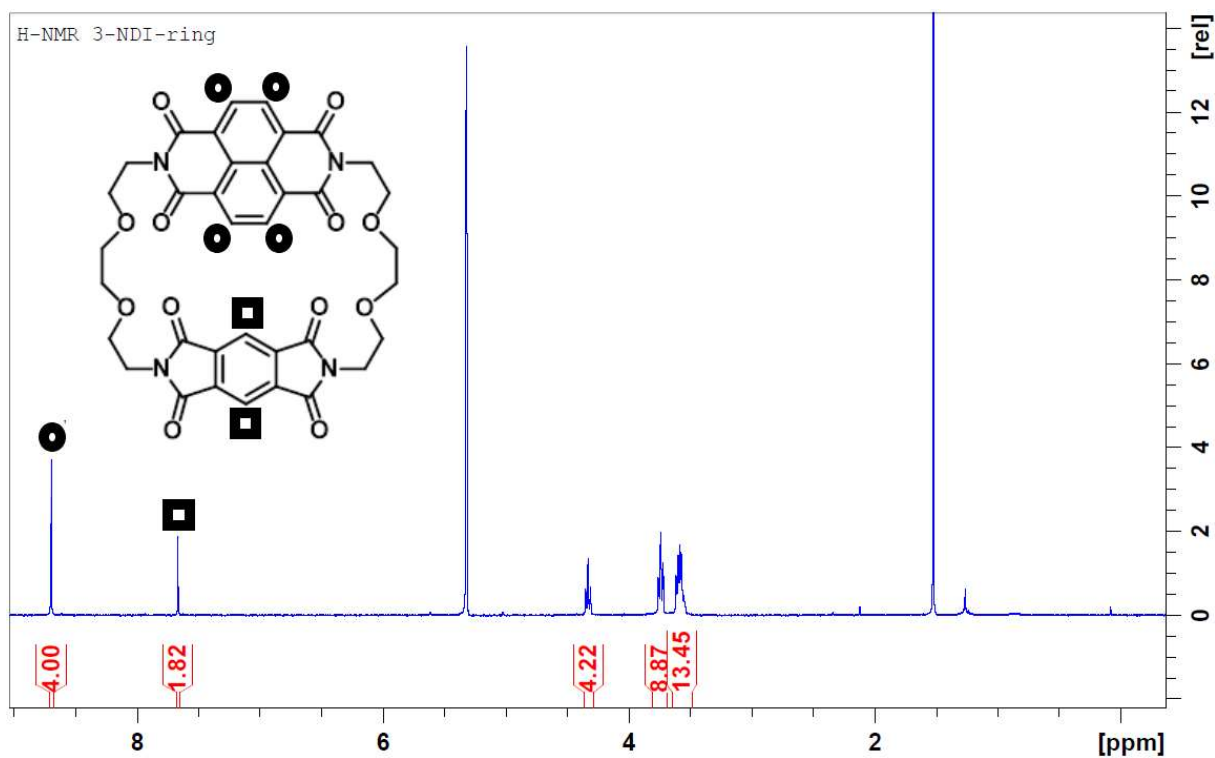
2.1 Synthesis of the 3-NDI Ring



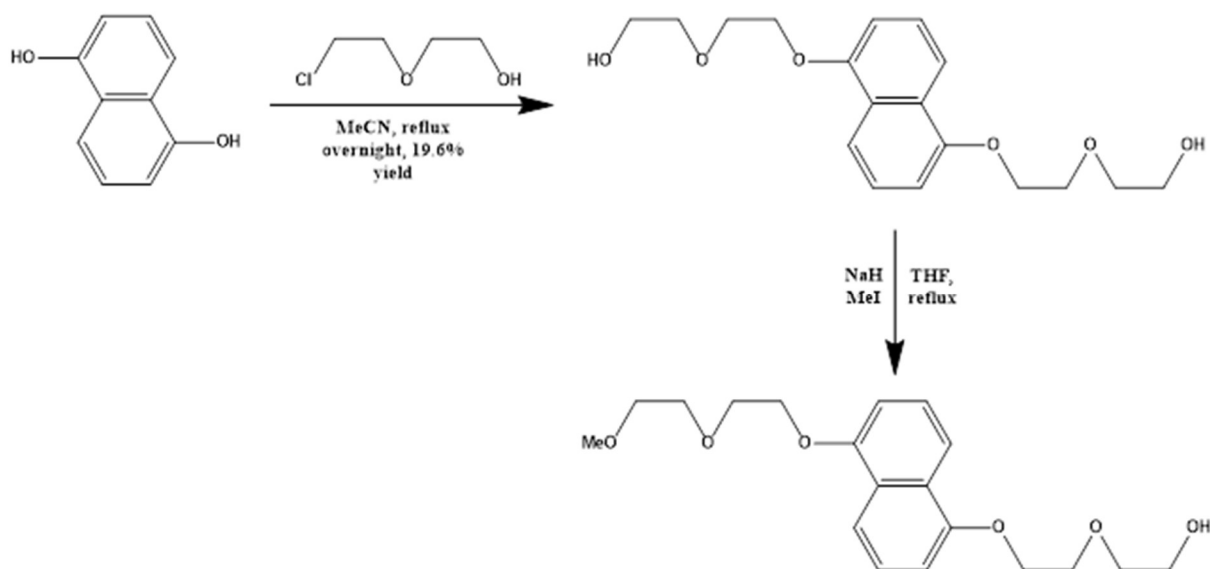
Scheme 1 Synthesis scheme of 3-NDI Ring

This synthesis strategy (**Scheme 1**, see also **Chapter 4.1** and **4.2**) makes use of a Mitsunobu alkylation for the cyclization step with naphthalene diimide (NDI-3) and pyromellitic diimide. NDI-3 is synthesized via a condensation reaction between commercially available naphthalene-tetracarboxylic dianhydride (NTDA) and 2-[2-(2-aminoethoxy)ethoxy]ethanol. The latter was already available, synthesized by the research group from a three-step synthesis from tetraethylene glycol with consecutively a tosylation, an azidation and an azide reduction. Pyromellitic diimide is commercially available and used without purification, 3-NDI Ring was synthesized and purified successfully, showing from the NMR spectrum (see **Figure 16**).

¹H-NMR (300 MHz, CD₂Cl₂) δ 8.65 (s, 4H, NDI-H), 7.60 (s, 2H, PDI-H), 4.33 (t, 4H, N-CH₂), 3.80 - 3.68 (m, 10H, 5 x CH₂), 3.65 - 3.55 (m, 14H, 7 x CH₂).



2.2 Synthesis of bis 2-(2-methoxyethoxy)ethanol-naphthalene and subsequent methylation



Scheme 2 Synthesis scheme of methylated naphthalene

In **Scheme 2** is reported the scheme of the synthesis of naphthalene with polyethylene glycol (PEG) side-chains, this naphthalene moiety is an electron rich aromatic system, allowing for electron deficient aromatic systems to coordinate to it via p-p interactions. It functions as the thread in a pseudorotaxane, with the redox mediator being the macrocycle **3-NDI Ring**. The first step is a Williamson's reaction for the synthesis of an asymmetric ether, starting from naphthalene 1,5-diol and two equivalent of 2-(2-chloroethoxy)ethan-1-ol. The second step is the methylation of the intermediate product, in presence of NaH as base and MeI as the methylating agent. The final product and the intermediate were characterized by NMR spectroscopy (**Figure 17** and **18**), where is shown the new signal, related to O-CH₃, at 3.39 ppm .

Intermediate) ¹H-NMR (300 MHz, CD₂Cl₂) d 7.89 (d, 2H, 2xCH), 7.39 (t, 2H, 2xCH), 6.88 (d, 2H, 2xCH), 4.34 (t, 4H, 2xCH₂), 4.03 (t, 4H, 2xCH₂), 3.79 (m, 8H, 4xCH₂).

Final product) ¹H-NMR (300 MHz, CD₂Cl₂) d 7.86 (t, 2H, 2xCH), 7.35 (td, 2H, 2xCH), 6.84 (d, 2H, 2xCH), 4.30 (t, 4H, 2xCH₂), 3.99 (t, 4H, 2xCH₂), 3.75 (m, 6H, 3xCH₂), 3.59 (m, 2H, CH₂) 3.39 (s, 3H, O-CH₃).

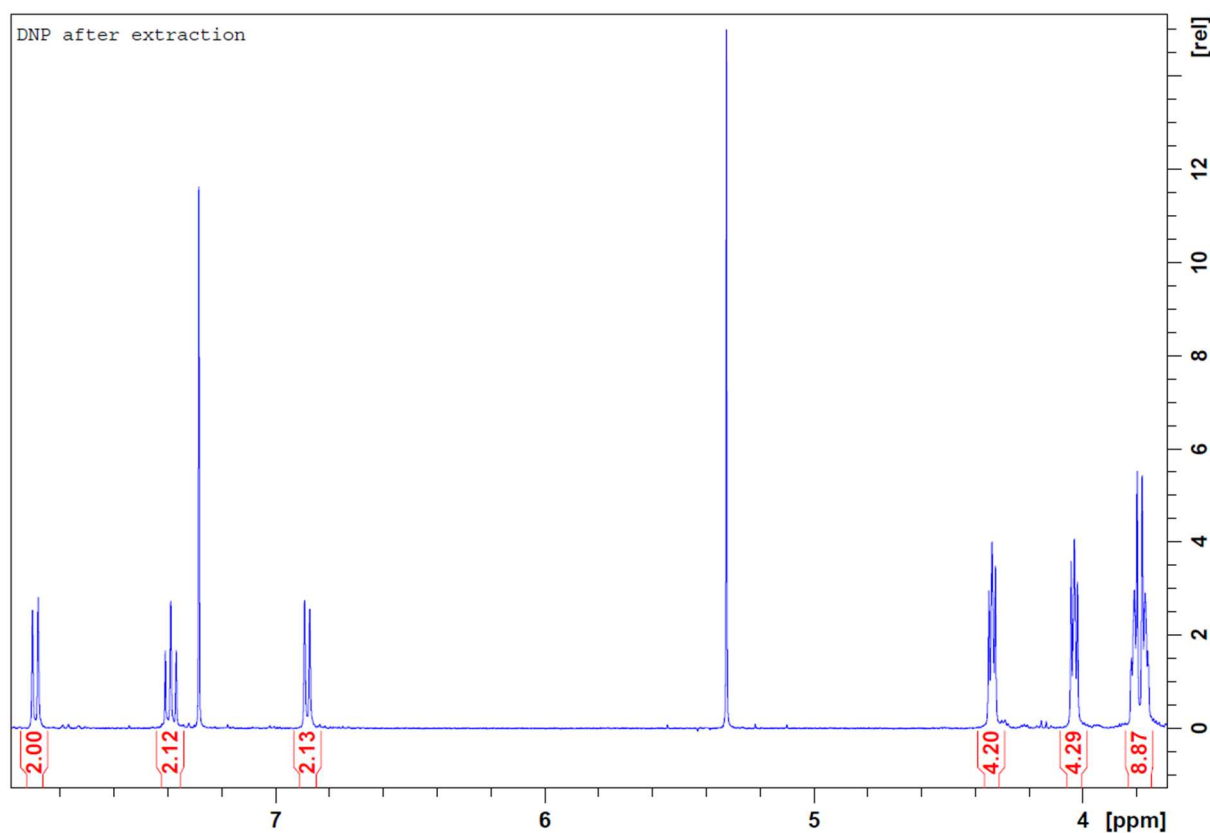


Figure 17 ¹H-NMR spectrum of intermediate naphthalene derivate

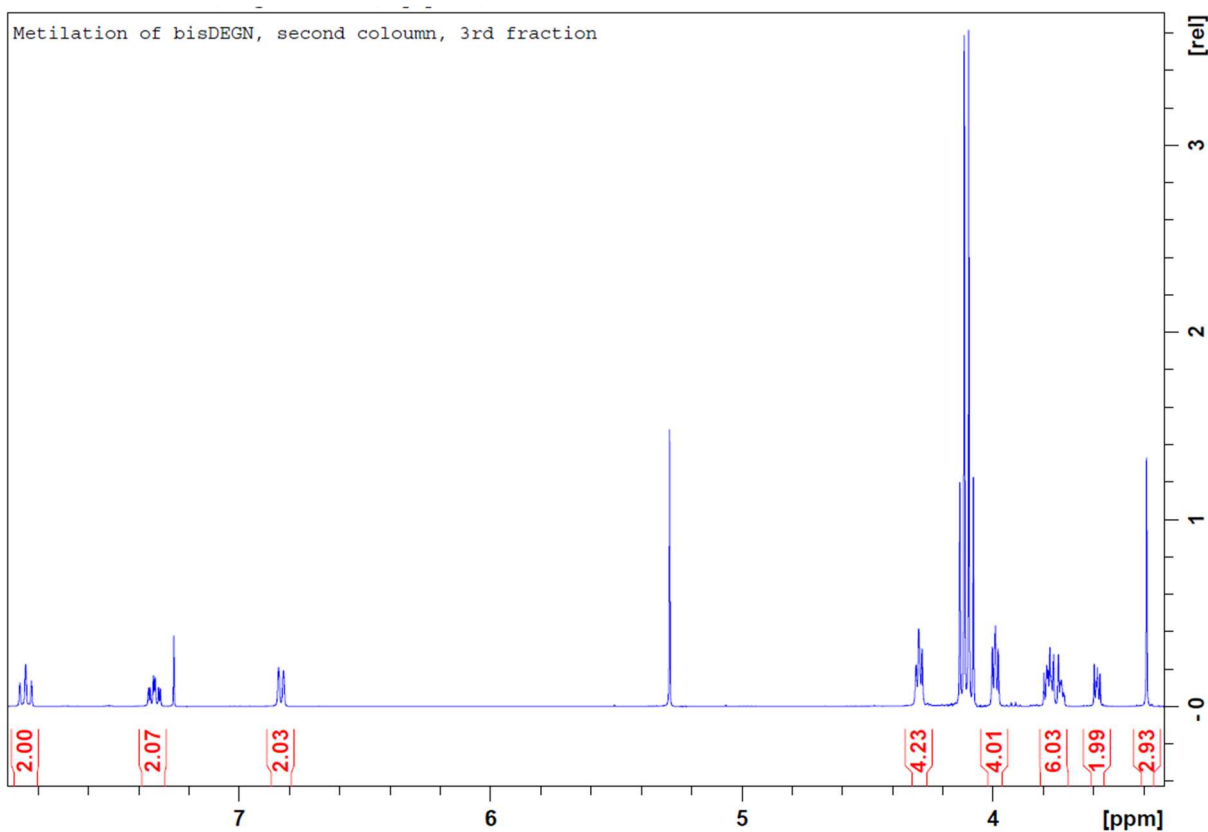


Figure 18 ^1H -NMR spectrum of methylated naphthalene derivate

2.3 Interaction between 3-NDI-ring and three different types of Dyes

Using a 2D-DOSY-NMR experiment is possible to quantify the diffusion constant (LogD) of a compound inside a mixture. Calculating the LogD of two isolated compounds, dissolved in a determinate solvent at fix temperature, comparing the value with the LogD calculated in a mixture of the two compounds, using the same solvent and temperature, is possible to determinate if is occurring an interaction. In **Table 2** are shown the molecules studied, the three dyes were synthetized by the research group. All the results are summarized in **Table 3**, only the PMI dyes shows an interaction with 3-NDI Ring, probably because the others two dyes (PDI and PMITPA), despite the same perylene moiety is present, are blocked at one side by the bulky groups (double imide for PDI and imide plus triphenylamine for PMITPA).

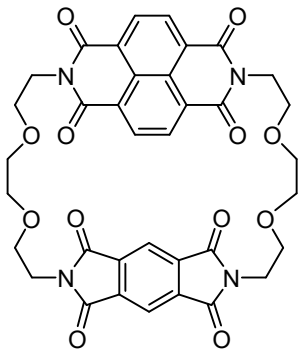
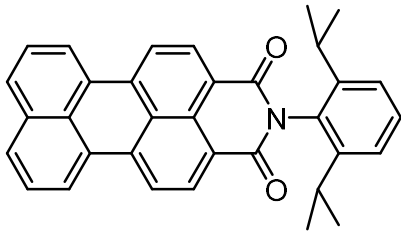
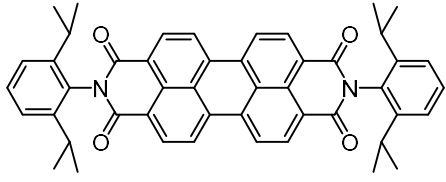
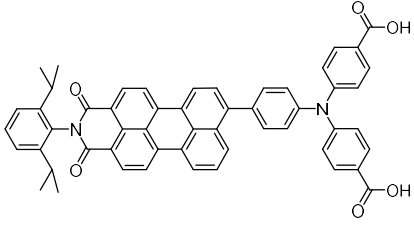
	
3-NDI-ring	Perylene-monoimide (PMI)
	
Perylene-diimide (PDI)	Perylene-monoimide-triphenylamine (PMITPA)

Table 2 Molecular structure of the studied molecules

Compound	Solvent	Conc. (mM)	LogD (Log(m ² /s))
3-NDI-ring	DCM	2	-8,77
3-NDI_ring	THF:DCM 1:1	0,5	-8,96
PMI	DCM	2	-8,86
PDI	DCM	1	-9,03
PMITPA	THF:DCM 1:1	2	-9,05
Ring + PMI	DCM	1 + 1	-8,88
Ring ^a + PDI ^b	DCM	0,5 + 1	-8,98 ^a ; -9,03 ^b
Ring ^a + PMITPA ^b	THF:DCM 1:1	0,5 + 1	-8,97 ^a ; -9,05 ^b

Table 3 LogD value of the free compounds and of the mixed solutions

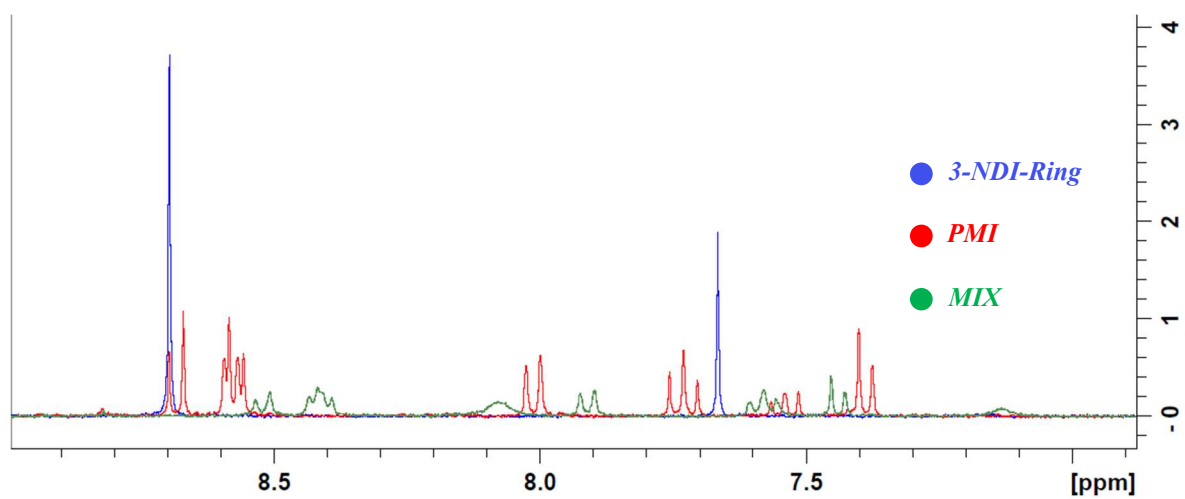


Figure 19 ¹H-NMR (7,0-9,0 ppm) 3-NDI Ring (Blue); PMI (Red); Mix (Green) in DCM

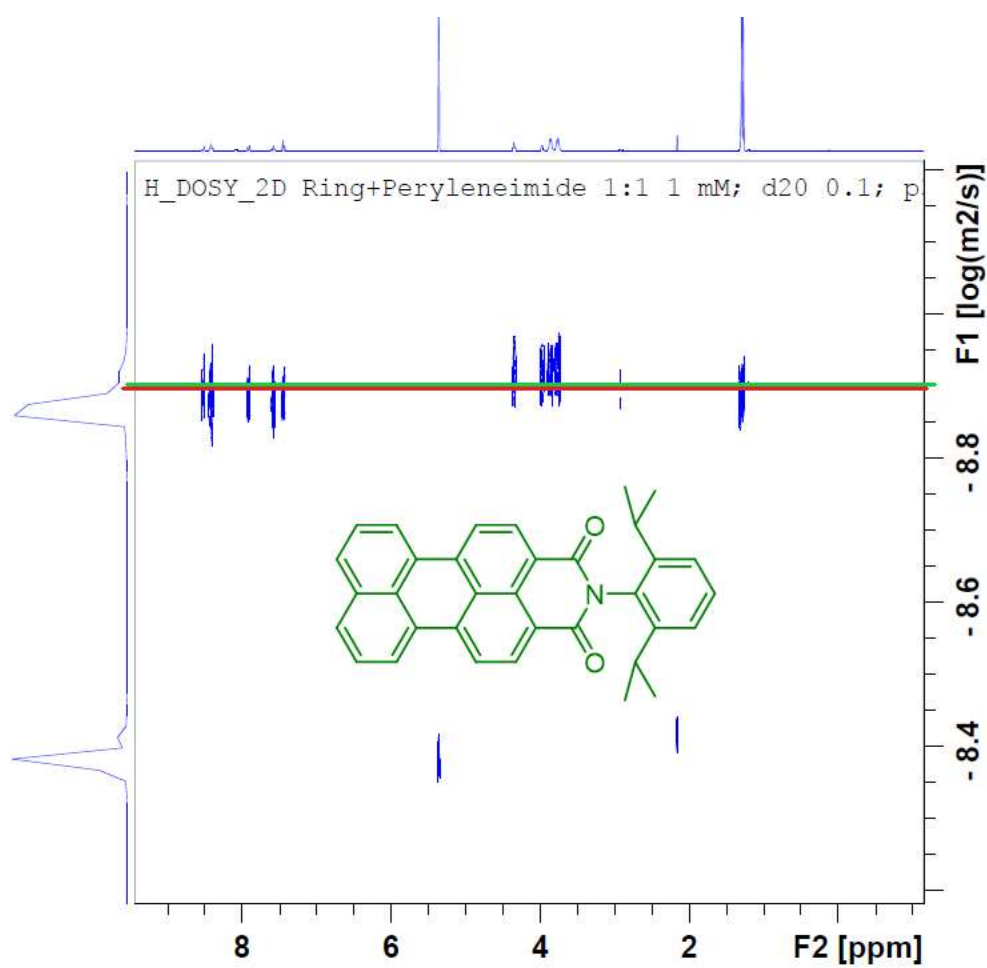


Figure 20 2D-DOSY 3-NDI Ring (Red line) + PMI (Green line) in DCM

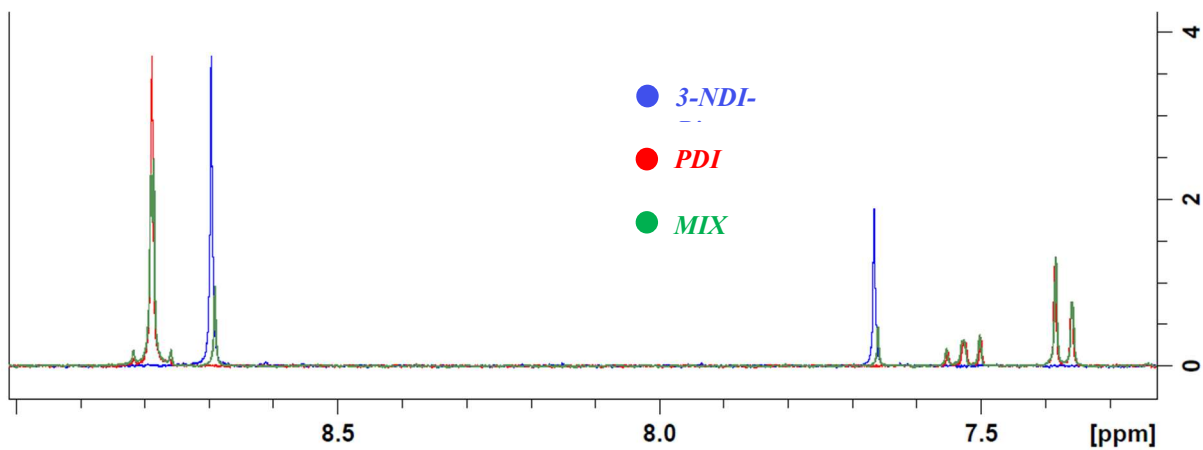


Figure 21 ¹H-NMR (7,2-9,0 ppm) 3-NDI Ring (Blue); PDI (Red); Mix (Green) in DCM

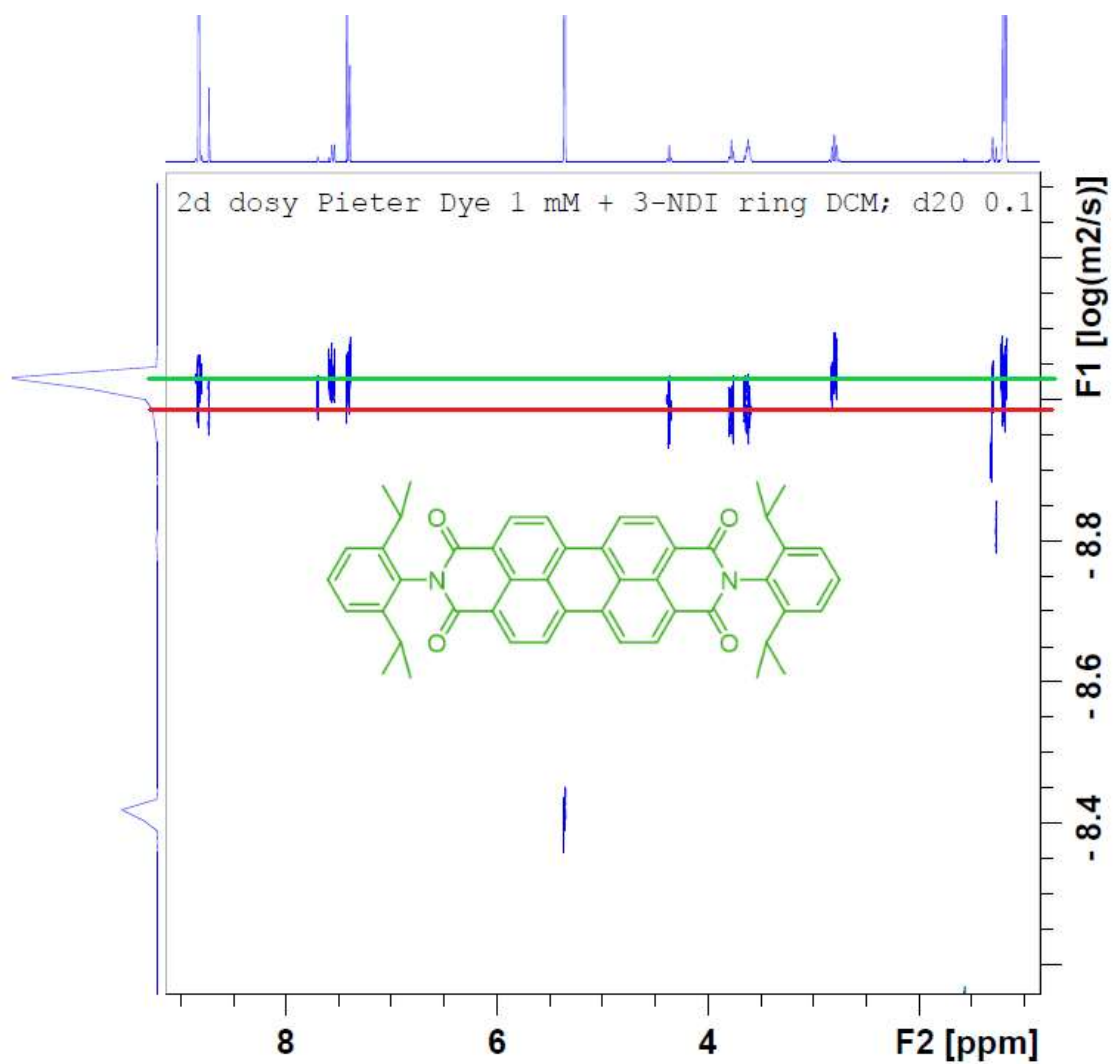


Figure 22 2D-DOSY 3-NDI Ring (Red line) + PDI (Green line) in DCM

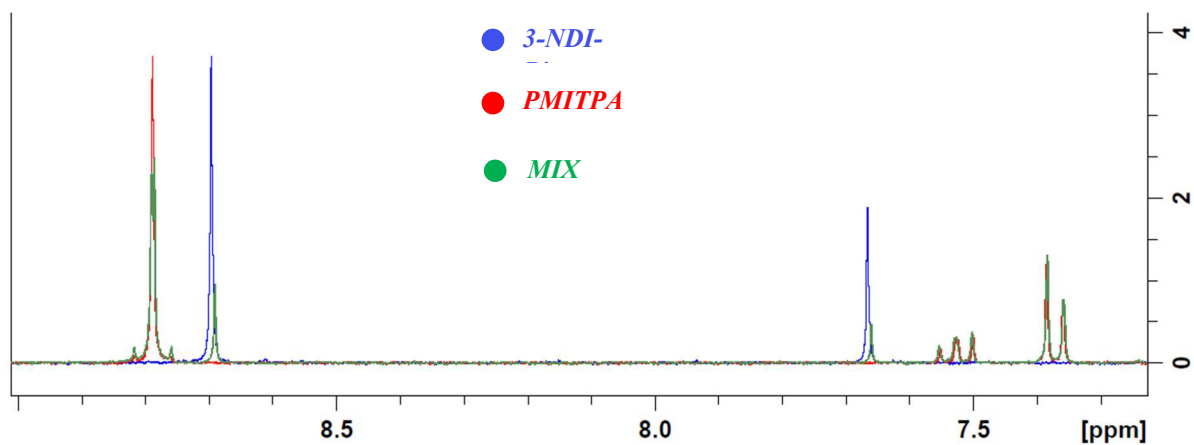


Figure 23 $^1\text{H-NMR}$ (6,8-8,8 ppm) 3-NDI Ring (Blue); PMITPA (Red); Mix (Green) in DCM-THF 1-1

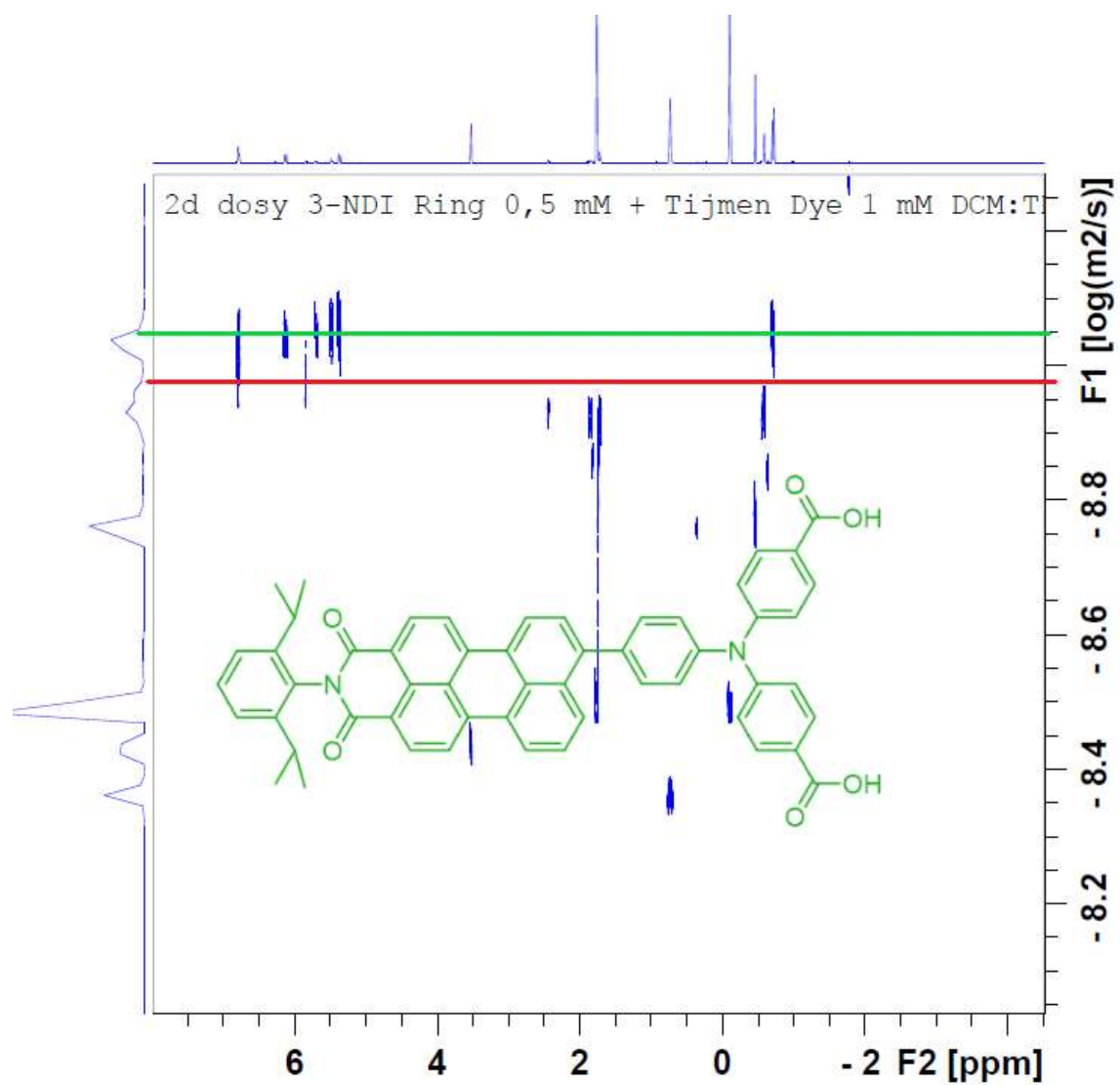
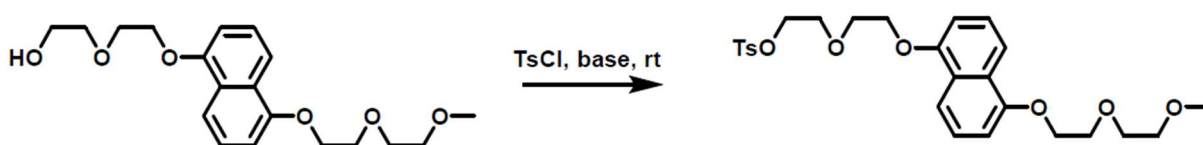


Figure 24 2D-DOSY 3-NDI Ring (Red line) + PMITPA (Green line) in DCM-THF 1-1

2.4 Future research

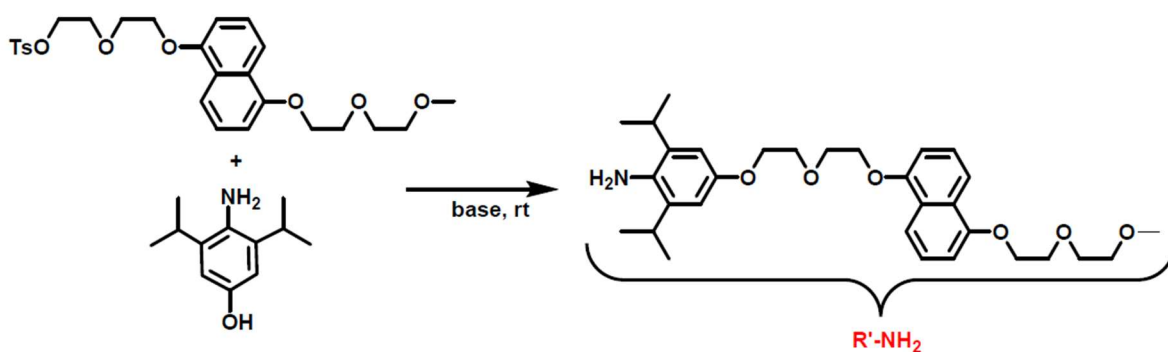
The work that I have done in the laboratory of Prof. Joost Reek was interrupted due to SARS-CoV-2 pandemic and my project did not accomplish the goals illustrated on the Aim of this thesis (See **chapter 1.7**). The planned path of the project is described below, where I have summarized the first steps I would have to face with.

After the synthesis of the methylated bis 2-(2-methoxyethoxy)ethanol-naphtalene, together with the help of my supervisors, we should have done the following synthesis:



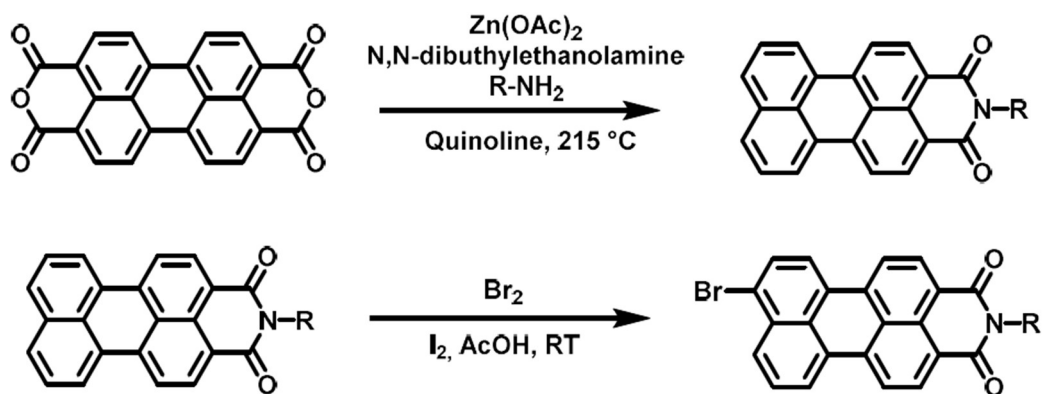
Scheme 3

The first step is the substitution of the poor leaving group -OH with the better TsO^- to give product B, this is the same Williamson's reaction used in the last step reported on **Scheme 2**.



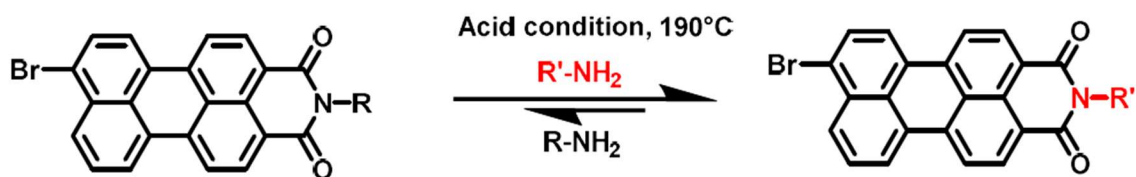
Scheme 4

Next step is another Williamson's reaction, starting from the previously synthesized naphthalene derivative (B) and 4-amino-3,5-diisopropylphenol (C) already available in the laboratory, synthesized by the research group. The product is an half part of the final dye, where the diisopropyl aniline moiety is the bulky group necessary to the construction of a push-pull dye (previously described in paragraph x), and the naphthalene derivative is the electron donor group.



Scheme 5

The second half part of the dye is the electron withdrawing group, obtained from modification on the Perylene-3,4,9,10-tetracarboxylic dianhydride (PTDA), first by reduction in presence of a not much bulky amine, obtaining the perylene-monoimide. Second step is the bromination of the product, necessary for the future anchoring on the NiO electrode surface.



Scheme 6

The final step is the exchange of the imide in Perylene, operated in strong acid and high temperature, resulting in the final structure desirable.

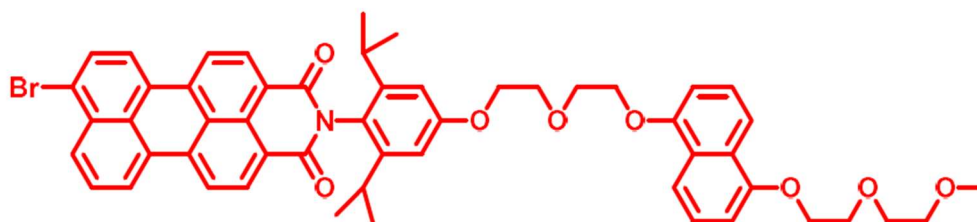


Figure 25 Final Structure of the dye

All the synthesis are not completely developed and the feasibility remains uncertain due to numerous doubts regarding the yield and specificity of some reactions.

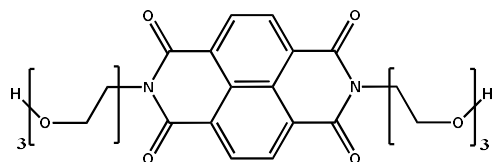
3 Conclusion

After studying the diffusion constants of the redox mediator (**3-NDI Ring**), three different dyes (**PMI, PDI, PMITPA**) and the possible interaction between them, it is possible to say that an interaction is observed only between **3-NDI Ring** and **PMI**. This is due to the structure of the dye which permits the insertion of the ring around the dye. The observed fact that there's no interaction between the other dyes can be described that there's only one way by which the ring can anchor the dye, surrounding it, although a planar π interaction could also occur.

Due to SARS-CoV-2 pandemic I was not able to continue this research and accomplish the synthesis of a new dye, based on the results obtained by studying the research group dyes. Thus, further research needs to focus on this synthesis and find the best optimization to avoid recombination events that decrease the power conversion efficiency of p-type dye sensitized solar cells.

4 Experimental section

4.1 Synthesis of 2,7-bis(2-hydroxyethyl)benzo[*lmn*][3,8]phenanthroline-1,3,6,8(2H,7H)-tetraone

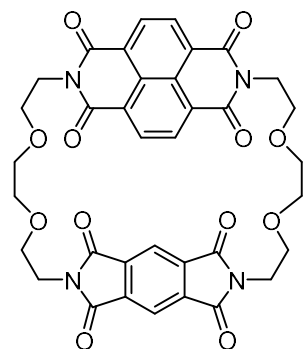


2-(2-(2-aminoethoxy)ethoxy)ethan-1-ol (1.5g, 10mmol) was dried by adding three times 0,5mL of toluene and removing the H₂O-toluene azeotrope using a rotary evaporator. Working in a N₂ atmosphere this

dried alcohol (1.08g, 7.24mmol) was added to 1,4,5,8-naphthalenetetracarboxylic dianhydride (0.50g, 1.9mmol, 1eq) developing a green/black mixture. This mixture was dissolved in DMF (15mL) resulting in a pale-yellow solution, which was stirred for 17 hours at 150°C giving a black suspension. After removing the solvent a black solid remained that was suspended in 20 mL CHCl₃ and 20 mL H₂O. The insoluble solids were filtered and the filtrate was extracted three times with 20 mL CHCl₃. A black solution formed in the organic layer, while the aqueous layer was clear. After drying the organic layer with MgSO₄ and removing the solvent a grey-black solid remained, Yield: 1.78g, 3.36mmol, 95.6%.

¹H-NMR (500 MHz, CDCl₃) δ 8.77 (s, 4H, NDI-H), 4.48 (t, J = 5.7 Hz, 4H, N-CH₂), 3.88 (t, J = 5.7 Hz, 4H, 2 x CH₂), 3.73 - 3.69 (m, 4H, 2 x CH₂), 3.65 - 3.60 (m, 8H, 4 x CH₂), 3.53 (t, J = 5.4 Hz, 4H, 2 x CH₂).

4.2 Synthesis of 3-NDI ring



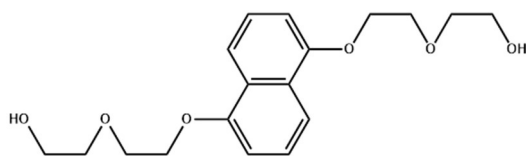
Working in a N₂ atmosphere, diol 1 (176 mg, 0.33 mmol, 1 eq), pyromellitic diimide (69 mg, 0.32 mmol, 1 eq) and PPh₃ (208 mg, 0.79 mmol, 2.3 eq) were dissolved in dried THF (25 mL). After adding DIAD (156 mL, 0.79 mmol, 2.3 eq) a grey suspension developed. After stirring this solution for 23h at room temperature the solvent was removed, The remaining grey- brown solid was suspended in 8 mL 19:1 DCM:MeOH in within it was stored for 2h,

This grey-brown suspension was filtered resulting in a brown solution and a grey solid, The

brown solution was purified by column chromatography (19:1 DCM:MeOH) resulting in a pink/red solid. Yield: 23mg, 32 mmol, 9,7 %. solid.

$^1\text{H-NMR}$ (300 MHz, CD_2Cl_2) d 8.65 (s, 4H, NDI-H), 7.60 (s, 2H, PDI-H), 4.33 (t, $J = 5.7$ Hz, 4H, N- CH_2), 3.80 - 3.68 (m, 10H, 5 x CH_2), 3.65 - 3.55 (m, 14H, 7 x CH_2).

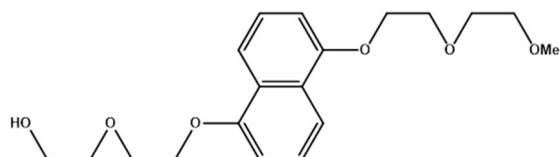
4.3 Synthesis of bis 2-(2-methoxyethoxy)ethanol-naphthalene



Working under N_2 atmosphere, K_2CO_3 (12g, 87mmol, 2.8 eq) and KI (1g, 6mmol, 0.2eq) were added to a 3-neck flask and flame dried under vacuum. Then 1,5 dihydroxy-naphthalene (5.014g, 31mmol, 1eq) were added together with 100mL of MeCN. After the solvent, 2-(2-chloroethoxy)ethanol (10.9mL, 125mmol, 4eq) were added into the reaction mixture and leaved stirring overnight at 100°C . The solution was filtered, washed with 10mL of DCM and dried under vacuum. The remaining black/grey solid was dissolved in 300mL of water and extracted with 600mL of EtOAc. The solution was dried under vacuum and purified through a silica plug using EtOAc first and then a MeOH:EtOAc (10:90) solution. After drying under vacuum a white solid result. Yield: 2,065g, 6.14mmol, 19.6%.

$^1\text{H-NMR}$ (300 MHz, CD_2Cl_2) d 7.89 (d, 2H, 2xCH), 7.39 (t, 2H, 2xCH), 6.88 (d, 2H, 2xCH), 4.34 (t, 4H, 2x CH_2), 4.03 (t, 4H, 2x CH_2), 3.79 (m, 8H, 4x CH_2).

4.4 Methylation of bis 2-(2-methoxyethoxy)ethanol-naphthalene



1g (2.98mmol, 1eq) of 2,2'-(((naphthalene-1,5-diylbis(oxy)))bis(ethane-2,1-diyl))bis(oxy))bis(ethan-1-ol) was dissolved in 14mL of dried THF, under N_2 atmosphere. Then NaH (0.1306g, 3.27mmol, 1.1eq) was added and the reaction was leaved stirring at 70°C . After 1h the solution was cooled to 40°C and MeI (0.195mL, 3.13mmol, 1.05eq) was added and the solution was leaved stirring overnight at 40°C . The reaction was quenched with 20mL of MeOH

and then dried under vacuum. The resulting white solid was purified through a silica chromatography column and the fraction containing the product was dried under vacuum. Yield: 0.23g, 0.66mmol, 22.1%.

$^1\text{H-NMR}$ (300 MHz, CD_2Cl_2) δ 7.86 (t, 2H, 2xCH), 7.35 (td, 2H, 2xCH), 6.84 (d, 2H, 2xCH), 4.30 (t, 4H, 2xCH₂), 3.99 (t, 4H, 2xCH₂), 3.75 (m, 6H, 3xCH₂), 3.59 (m, 2H, CH₂) 3.39 (s, 3H, O-CH₃).

Chapter II

Abstract

During my training period I synthesized new Fe(0) cyclopentadienone compounds bearing a N-Heterocyclic Carbene ligand. The aim of the thesis was to achieve water solubility by modifications of the cyclopentadienone ligand. These new complexes have been modified using a sulfonation reaction, replacing an hydroxyl with a sulfate group, on the alkyl backbone of the cyclopentadienone ligand. All the complexes were characterized with IR, ESI-MS and NMR spectroscopy, and a new Fe(0) cyclopentadienone complex, involved as an intermediate, was obtained as a single crystal and was characterized also with X-Ray spectroscopy.

1. Introduction

In last decades, sustainability has emerged as a new paradigm in scientific research as response to the major economic, environmental and social challenges facing our society. Indeed, meeting future energy demands, reducing pollution, minimizing waste releases, reducing the use of essential raw materials or finding substitutes etc., can only be solved through a sustainability based approach. Many concepts, ideas and theories have developed about the central role that chemistry can play in order to address the above mentioned challenges.

One of the emerging sustainability concepts emphasize the use of environmentally benign, earth abundant and inexpensive first row transition metals such as iron instead of the traditional second and third row transition metals. This has a major impact in the area of transition metal homogeneous catalysis, in that the most relevant advances were obtained (so far) using noble transition metals such as palladium, rhodium, platinum, iridium, which are toxic, rare and cannot sustain large scale applications. Replacing these noble metals with iron, maintaining excellent catalytic properties, is very challenging and implies a new approach to the metal – ligand design. For example, many efforts in the research of catalytic iron based substitutes are inspired by natural occurring enzymes. Indeed, nature widely uses non precious metals to perform specific and high efficient catalysed reactions with the help of powerful ligands. Cooperation between ligands and metal centre is the key prerogative in order to exploit earth abundant metals. In the bio-inorganic field, bio-mimetic compounds have been developed to be employed as drug in treating the most dangerous disease.

In the following introduction, the first part will be focused on an overview of non-innocent ligands, which inspired the design of a new class of iron compounds described in this thesis, then it will wove to the discussion focus on the capability of this complexes to perform catalysis in aqueous solution thanks to the modifications on their ligands.

1.1 Non innocent ligands

Non innocent ligands (NILs) are redox-active molecules, which can be used to easily tune the electronic properties of a metal complex. The term non innocent ligands was first defined by C. K. Jørgensen in 1966, who was trying to better understand the oxidation states of metal centres:

“Ligands are innocent when they allow oxidation states of the central atoms to be defined. The simplest case of suspect ligand is NO”.¹

In nature, NILs are extensively exploited to perform multi-electron reactions with Earth-abundant base metals (e.g. Fe, Cu), which involve a single electron event. On the contrary, in homogeneous catalysis precious noble metals (e.g. Ru, Rh, Ir) are utilized, since they undergo a $2e^-$ oxidation state changes, thus they are able to easily perform two-electron processes.

In this point of view, NIL is a useful tool to imitate a noble metal, but exploiting more Earth-abundant and cheaper first row base metals.²

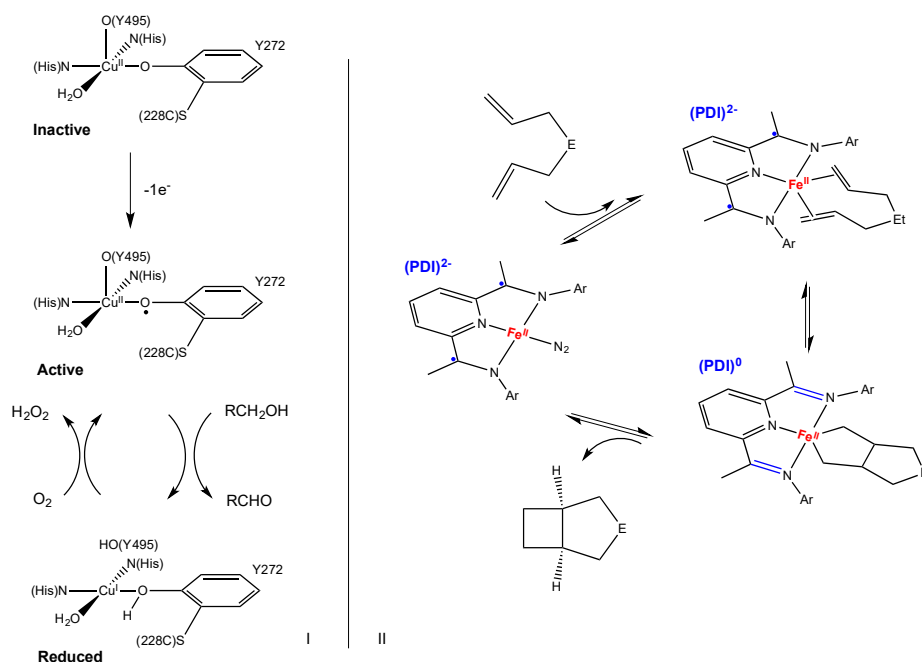
Non innocent activity can be divided in two main behaviours:³

- A. Spectator ligand, which influences the metal atom, that is the reactive site, either accepting or releasing electron from and to the metal atom.
- B. Actor ligand, which interacts directly with the substrate by forming or breaking bonds.

On this basis, four main approaches may be employed to take advantage of NILs:

1. Reduction/oxidation of the ligand to modify the Lewis acidity of the metal;
2. “Electron reservoir”, accepting and donating electron density from the ligand to the metal in order to avoid uncommon and high-energy oxidation state of the metal;
3. Radical generation on the ligand to actively participate in breaking/forming new bonds;
4. Radical generation on the ligand and transfer to the substrate to activate it and modify its reactivity.

Approaches 1 and 2 are typical of type A ligand, whilst 3 and 4 of type B one.



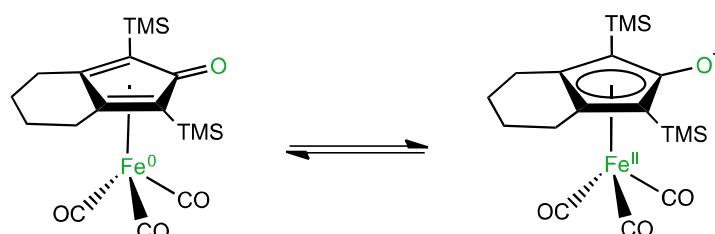
Scheme 1 On the left the Cu centre of galactose oxidase in the active ($\text{Cu}^{\text{II}}/\text{Y272}\bullet$) and reduced ($\text{Cu}^{\text{I}}/\text{Y272}$) form. On the right the PDI-iron complex with different oxidation levels of the non-innocent ligand. The E indicates any alkyl group.³⁻⁷

The use of NILs in metal complexes draws inspiration from enzymes in nature. One example is the galactose oxidase (GOase), a Cu^{II} centre which is able to perform a two electron oxidation of alcohols to aldehydes.⁴ The active site is made up of a Cu active site coordinate to two histidine and two tyrosine residues (**Scheme 1**).⁵ Activation goes through addition of one electron to a tyrosine to form a tyrosyl radical. The reduced form is made of a Cu^{I} site and a tyrosinate residue, which is then oxidized by an oxygen molecule back to the active form. Notably, the one-electron couples $\text{Cu}^{\text{I}}/\text{Cu}^{\text{II}}\text{-Y272}/\text{Y272}\bullet$ are able to perform a two-electron overall oxidation; this is an example of a redox-active ligand of type B, where the ligand is directly involved in breaking bonds.

An example of type A NILs is the synthetic bis(imino)pyridine-type ligand (PDI), where four different oxidation levels are permitted: neutral, mono-, di- and tri-anions. The well-defined (PDI)- Fe^{II} complex developed by Brookhart et al. and Gibson et al. is able to polymerize olefin⁶ as well as to perform other catalytic reactions such as hydrogenation and hydrosilylation. Notably, in the example reported in **Scheme 1-right**,⁷ a cyclization of diynes, electrons are shuttled from and to the PDI ligand without changing the oxidation state of the iron centre.

1.2 Iron Cyclopentadienone complexes

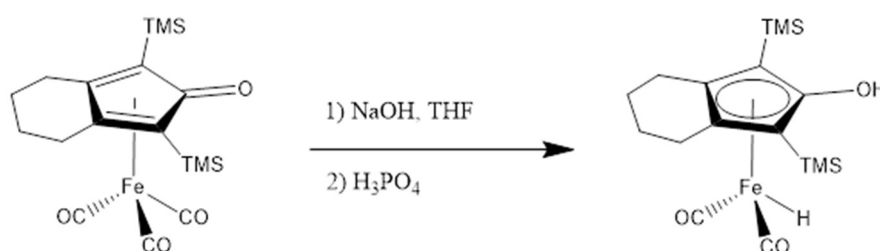
One of the most famous and employed catalyst bearing a non-innocent ligand is the Shvo's ruthenium catalyst,⁸ discovered in middle 1980s and known for its robustness and versatile activity in hydrogenation of polar double bonds. Its mechanism implicates a simultaneous transfer of separated hydrogen atoms from the metal centre and the ligand, which is known as ligand-metal bifunctional catalysis. Indeed, the Knölker's iron analogue⁹ is highly attractive considering the use of less expensive and toxic iron. The two possible species of iron complex, due to the ambiguity of the oxidation state of the iron centre, confirm the non-innocent nature of the ligand, which might be classified as an "electron reservoir" (**Scheme 2**).



Scheme 1. The possibility of representing the Knölker's iron complex as Fe⁰ or as Fe^{II} corroborates the non-innocent nature of cyclopentadienone ligand.

This class of iron complexes was first discovered in 1953, when Reppe and Vetter studied the reactivity of iron carbonyls with acetylenes, but were not able to identify this new species. Only six years later, Schrauzer¹⁰ found the structure of an iron(0) tricarbonyl complex bearing a cyclopentadienone ligand, coordinated by two π -interactions. Moreover, the electronic and steric properties of cyclopentadienone can be easily designed providing appropriate substituents (e.g. electron withdrawing or donating group on the alkyne).

In 1990s the complexes were employed to access the high value free cyclopentadienone ligands, until Knölker discovered the first Fe-hydride species:¹¹ Treating iron tricarbonyl precursor with aqueous NaOH, followed by acidification with H₃PO₄, which is a Hieber-type reaction, yielded an iron hydride hydroxycyclopentadienyl complex.



Scheme 3 Synthesis of Knölker complex Fe-II starting from Fe-I precursor

The new Knölker complexes were exploited by Casey et al. in 2007,¹²⁻¹³ as catalyst in the efficient hydrogenation of polar double bonds (e.g. ketones, aldehydes and imines) either by dihydrogen molecule or 2-propanol as hydrogen donor.

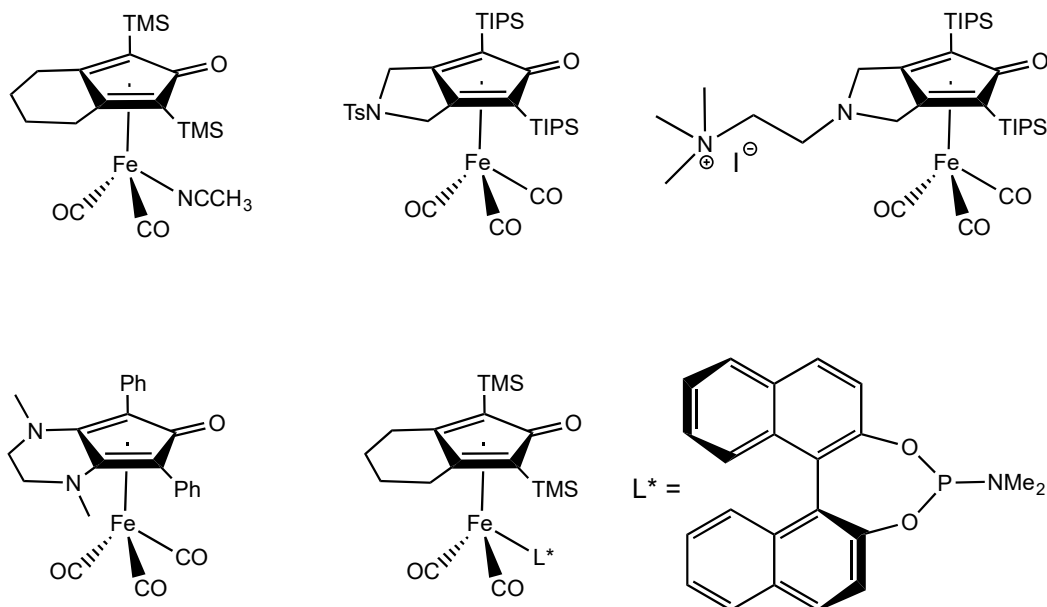


Figure 1. Structures of some modified iron compounds inspired by Knölker's iron complex. TMS, trimethylsilane; TIPS, triisopropylsilane, Ts, tosylate.¹⁵⁻¹⁶

Since Casey's discovery, the Knölker complex has been used extensively¹⁴ in several hydrogenations, oxidations as well as challenging dual catalysis. Another challenge is the functionalization of the iron complex in order to modify its reactivity and electronic properties: so far, this has been achieved either by changing substituents on cyclopentadienone or upon replacement of a carbonyl with another ligand.

For instance, Renaud's group focused on various cyclopentadienones¹⁵⁻¹⁶ and synthesized a bench-stable catalyst by displacement of carbonyl with a more labile acetonitrile.¹⁷ Berkessel et al. introduced a chiral phosphoramidite, obtaining the highest enantiomeric excess of 31%ee in the hydrogenation of acetophenone.¹⁸

Concerning this topic, good candidates in substitution of a carbonyl are N-Heterocyclic Carbenes, well-known universal ligands in organometallic chemistry.

1.3 N-Heterocyclic Carbenes

Carbenes are a 6-electrons divalent carbon compounds, which have two non-bonding electrons on the carbene carbon.¹⁹⁻²⁰

Their isolation, as free compounds, was actively pursued since the mid 1900s. In 1964 Fischer²¹ isolated the first stable carbene complex characterized by an electrophilic carbon; a few years later in 1974, Schrock²² isolated another type of carbene complex, but with a nucleophilic carbon. Both these complexes are now well-known as Fischer- and Schrock-type carbenes.

In between these two paramount discoveries, Wanzlick²³ and Öfele²⁴ reported autonomously the first N-Heterocyclic Carbene (NHC) complexes in 1968. The very explosion of the NHC as ligand in Organometallic chemistry started with the isolation of the first stable and “bottleable” carbene reported by Arduengo²⁵ et al. in 1991. The unexpected stability of NHC was thoroughly studied by several groups in order to shed some light on this species.

A carbene is a X₂C centre that might be linear or bent: the linear form is described as a triplet, whilst the bent can be either singlet or a triplet state (**Figure 2**).²⁸ The electronic configuration of these systems are strongly influenced by the α -substituents.

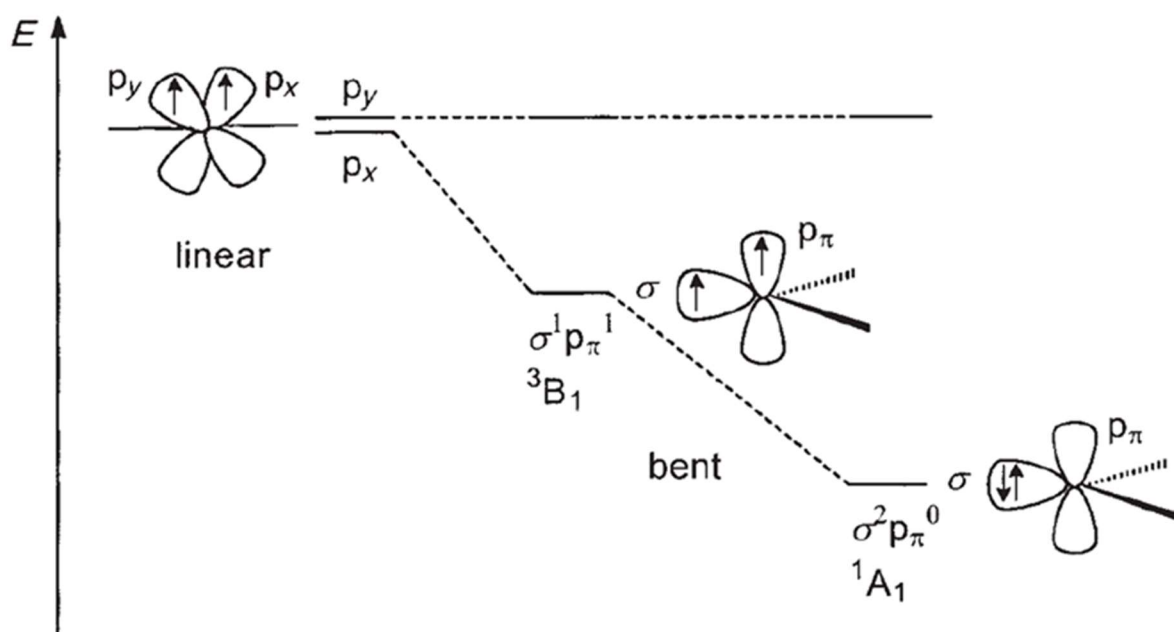


Figure 2. Diagram with energy of a linear carbene in a triplet state, and a bent carbene in a triplet 3B_1 or singlet 1A_1 . Calculations have shown that an energy gap of 2eV is required to stabilize the singlet A.²⁸

NHC is a X2C bent centre, where the carbon adopts a sp^2 -hybridised form in a singlet ground state configuration. The singlet state is well-described as a highest occupied molecular orbital (HOMO) sp^2 -hybridised lone pair, and a lowest occupied molecular orbital (LOMO) p-orbital on the C atom (**Figure 3**).²⁷

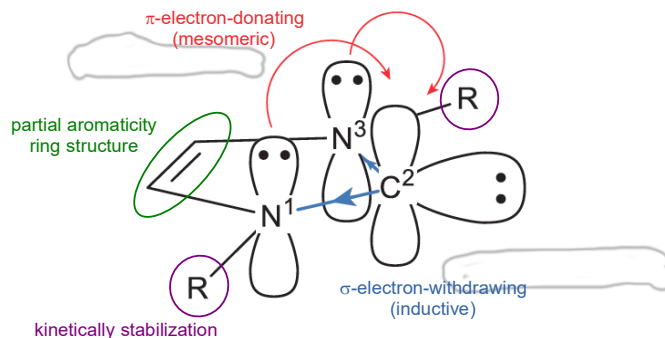
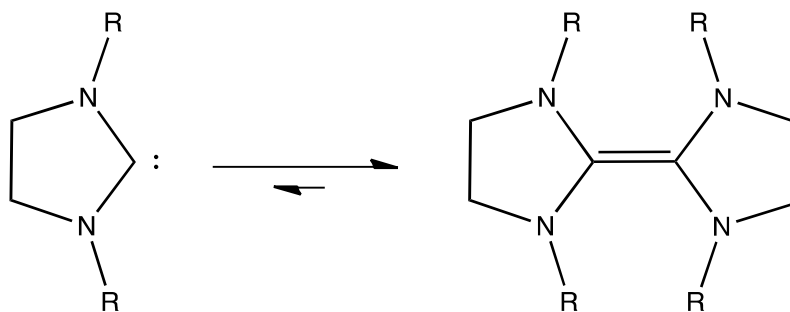


Figure 3. A representative carbene, where R is an alkyl or aryl substituent, N the nitrogen atoms and C the carbene carbon centre. All the features that make the NHC a stable compound are here summarised: the inductive and mesomeric effect of nitrogen atoms; the partial aromaticity due to the backbone; the kinetic stabilization by hindered R groups; the ring size, which forces the carbene centre to a bent form.²⁷

The electronic stabilization of the singlet is provided by the α -nitrogen atoms due to a double role: inductively, the sigma withdrawing effect stabilizes the non-bonding lone pair lowering the energy of the σ -orbital (HOMO); mesomerically, the donation of the π -amino lone pair into the vacant $p\pi$ -orbital, increases the energy of the empty p-orbital. Furthermore, the incorporation of the X2C centre into a five-membered ring forces the bent sp^2 -arrangement. Another source of stability is the partial aromaticity due to the backbone, which has been calculated to be about 25 kcal mol^{-1} , and this explains why also the simplest di-methyl-substituted NHC (Ime) is persistent in solution.

Concerning the R substituent on the heteroatoms, bulkier functional groups allow a kinetic-stabilization of the NHC, avoiding the dimerization into the olefin: this phenomenon is known as Wanzlick equilibrium.



Scheme 2. The Wanzlick equilibrium involves the free carbene (on the left) and its corresponding dimer, an olefin (on the right). The equilibrium is far to the right.

The NHCs are stable to air, but they must be stored under argon atmosphere due to hydrolysis. Water reacts with NHC by cleavage of C-N bond, yielding acyclic products.²⁸

These properties are general and apply to all NHCs, even though there are little variations due to the specific kind of compound. (**Figure 4**)

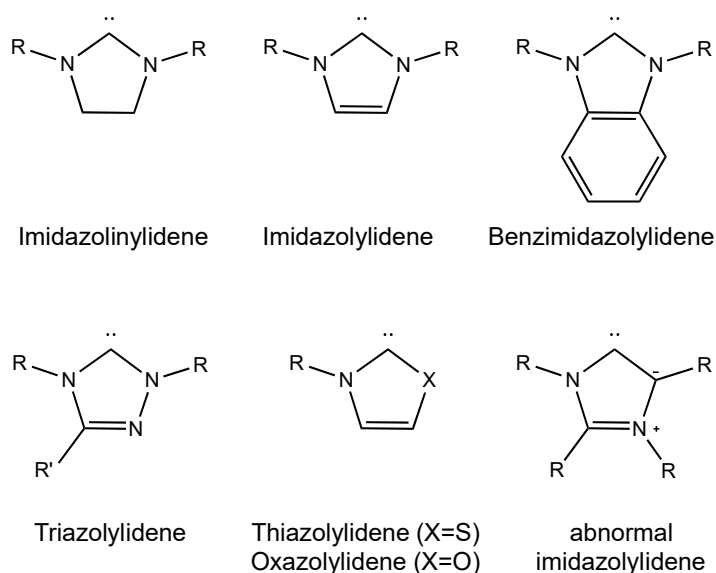


Figure 4. Some of the most common carbenes that have been applied in coordination chemistry and catalysis. R is any alkyl or aryl groups.

1.3.1 Electronic and steric properties

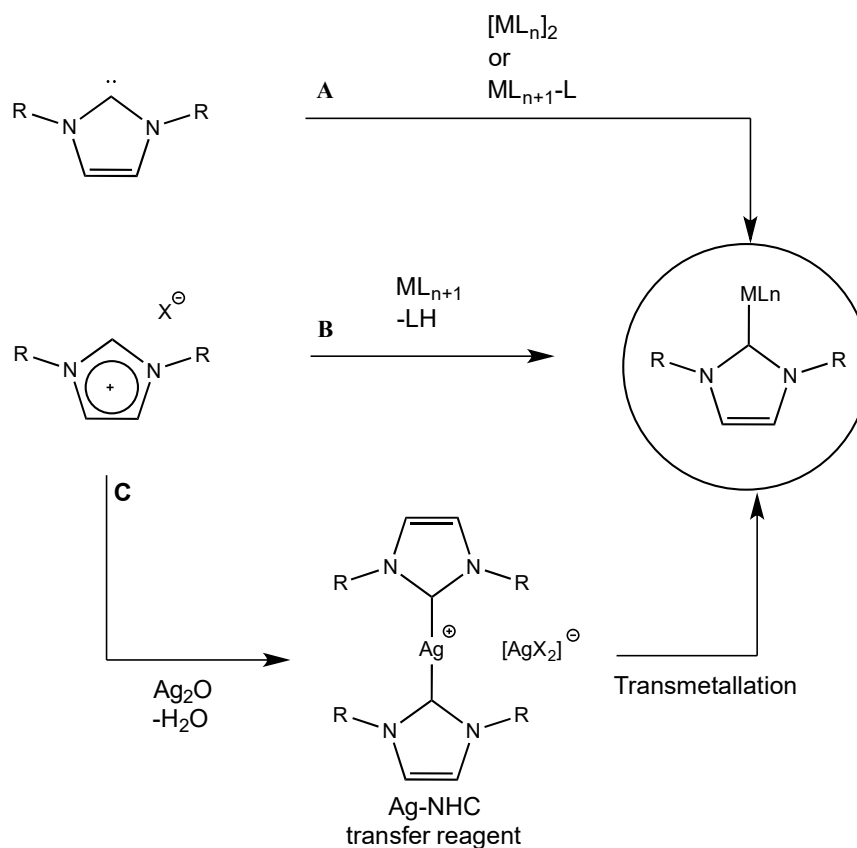
The electronic configuration of NHCs allows to understand their properties: the lone pair lying on the ring plane makes the NHCs a good ligand, which implies strong σ -donor ability. Therefore, NHCs provide a good alternative to the well-known phosphines. Both of them are sterically and electronically tunable, but with strong differences.

In phosphines, the R substituents are directly linked to the donor atom (P), thus a change on the R groups will change both the steric and electronic properties. Conversely, in the NHC, the R groups are far away from the donor central atom (C), having strong effects on the steric properties but a limited influence on the electronic properties. Changes of the electronic properties are usually obtained by modifying the nature of the ring.²⁹

Both electronic and steric features of NHCs make the resulting metal complexes more thermally and oxidative stable compare to the phosphine-metal compounds.³⁰

1.3.2 The nature of Metal-NHC bond

NHCs act as 2 electrons σ -donor neutral ligands and they strongly coordinate to metal leading to relatively stable NHC-metal complexes. The most useful methods to prepare these metal complexes are shown below. (**Scheme 5**)



Scheme 3. The most common methods to prepare NHC-metal complexes. L_n , ligand, X, halogen, R any alkyl or aryl groups.

- Reacting the free stable carbene with metal complexes.
- Reacting the imidazolium salt precursor with a metal compound bearing ligand acting as a base.
- Reacting silver oxide (Ag_2O) with the imidazolium salts yields the corresponding silver(I)-carbene complex, which is a special NHC-transfer reagent³¹ to other transition metals. This last route can be really useful in case of functionalized imidazolium salt with sensitive substituents.

Several X-ray structures of metal carbenes are now available. A big difference between a conventional carbene and a NHC is the M-C² bond distance, which is longer (>210 ppm) in the classical ones and lower in NHCs (<200ppm); this is due to the back-bond character of the NHC and reflects the possibility of rotation around the M-C² bond axis, depending on the steric environment. Indeed, as shown in **Figure 4**,³² the NHC is not a simple σ -donor, but the three orbital contributions in bonding involve also a π -NHC to d-M donation and a d-M to π^* -NHC backdonation.

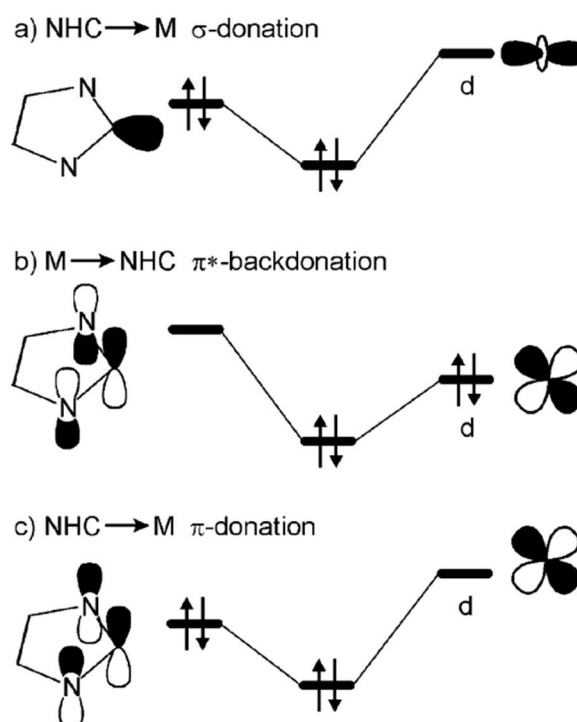
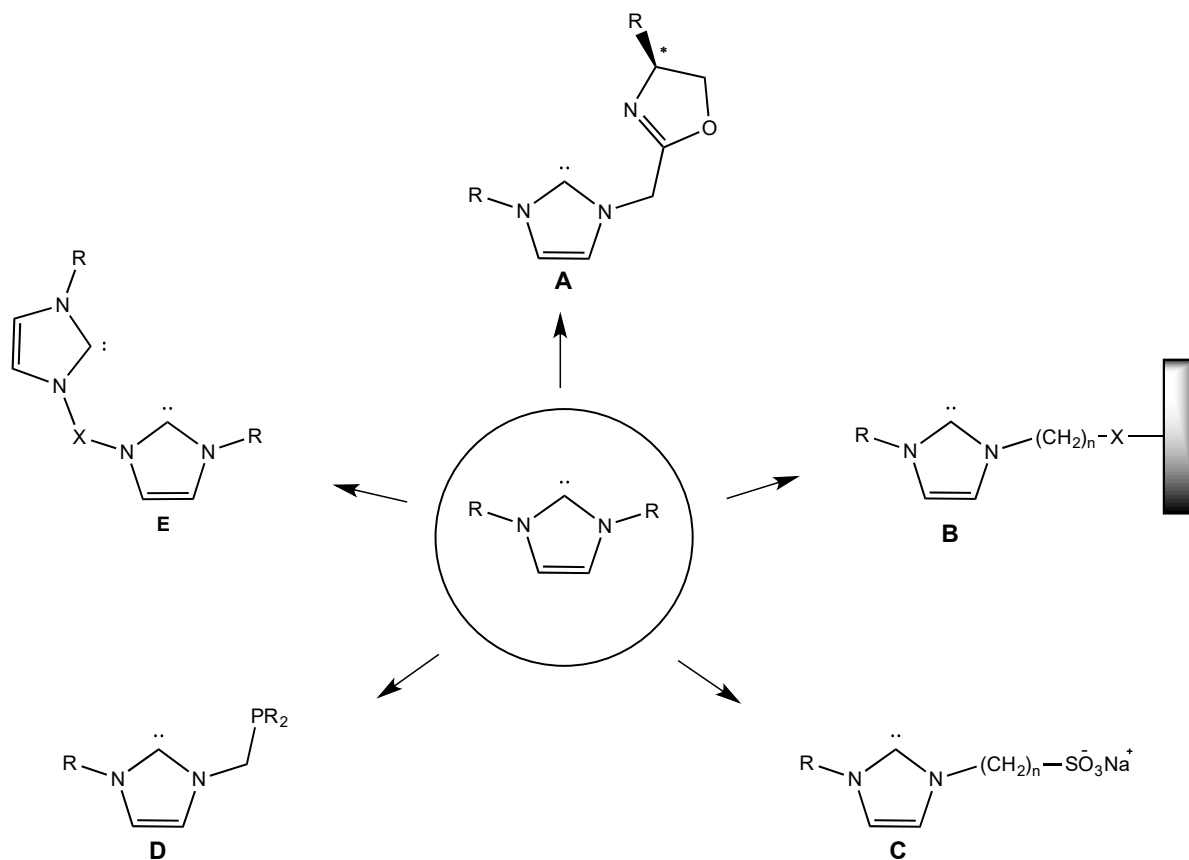


Figure 3. The three different contributions of NHC-M bond. a) sigma donation from carbene to metal centre; b) π -backdonation from d-orbitals of the metal to the π^* of the carbene; c) π -donation from π fo carbene to the d-orbitals of the metal.³²

NHC binds strongly to metal centre. Indeed, it has been demonstrated by DFT⁴¹ that M-CX₂ bond is about 44-45 kcal \times mol⁻¹, far more than M-PR₃ bond, which is about 25-37 kcal \times mol⁻¹. This bond prevents ligand dissociation in metal catalysts even in harsh conditions (eg. high temperatures, strong pH).

In addition, versatility in synthesis of NHC might be a big advantage in many applications (**Scheme 6**)³³: chirality, immobilization on solid support, water solubility of hydrophobic starting compounds, functionalization on the alkyl chain and chelate effect on metal center.



Scheme 4. Attractive features of NHC as ligands for organometallic compounds: a) chirality, b) immobilization, c) water solubility, d) functionalization and e) chelate effect. R, alkyl or aryl groups.³³

1.4 Catalysis in aqueous environment

Since the discovery that metals play a crucial role in several bio-relevant reactions, coordination compounds, including organometallic complexes, have been used in medicine as both diagnostic and therapeutic agents.³⁴⁻³⁵ One area that has certainly received a significant attention is the application of coordination and organometallic complexes as drugs or prodrugs in the cancer treatment.³⁶⁻³⁷ The readily available and inexpensive iron is a good candidate as a key component in many important biological processes,³⁸ and ferrocene derivatives are among the most studied iron complexes for their bioinorganic properties related to their reactivity and electrochemical properties.³⁹⁻⁴⁰ The presence of side-chain amino groups on ferrocifen

complexes leads to major toxicity,⁴⁰ similar to the one observed with other metallocenes.⁴¹ The current state-of-the-art reveals that the design of iron complexes containing ligands able to tune both their solubility in water and electronic properties is still a challenge for the development of bio-active organometallic compounds.

Within this field, the research group where I worked recently developed a straightforward pathway toward the synthesis of a new family of iron(0) complexes where the combination of cyclopentadienone (CpO), N-heterocyclic carbene (NHC) and carbonyl ligands were exploited.⁴²

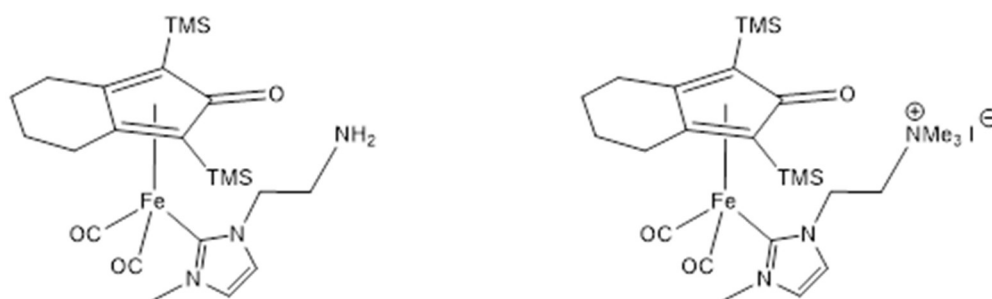


Figure 4. Fe (0) cyclopentadienone complexes containing cyclopentadienone ligands and N-heterocyclic carbenes

The complex on the right in **Figure 5**, thanks to the quaternary amine modifications on the NHC ligand, was found to be soluble in an aqueous environment, particularly in physiological conditions (buffer solution at pH 7.4). Anyway, best cytotoxic activity was registered for the amino functionalized complex (**Figure 5** left) in a DMSO/buffer solution mixture. The synthesis of new Fe(0) cyclopentadienone NHC complexes, in which the ligands allow to modify the solubility properties, is thus still an open challenge in the field of organometallics, the development of which opens the door to biological applications.⁴³ Furthermore, from a different point of view, the development of novel water soluble Knölker type iron complexes bearing NHC could be exploited in water homogeneous or biphasic catalysis, aiming to the use of sustainable solvent and/or to the recovery and reuse of homogeneous catalysts.

1.5 Aim of the thesis work

During my traineeship I worked under the supervision of Prof. Rita Mazzoni at the University of Bologna, after a period at the University of Amsterdam under the supervision of Prof. Joost Reek.

In Bologna I continued the research project focused on developing water soluble Fe(0) complexes able to act in eventual bio-inorganic applications or as catalysts under aqueous phase. Following the results obtained by the research group, as showed above in the 1.4 paragraph, the design, synthesis and characterization of new Fe(0) cyclopentadienone NHC complexes, with the aim of increasing water solubility without affecting electronic and steric properties of the metal center, was performed by modifications on the alkyl backbone of the cyclopentadienone ligand through a sulfonation reaction, operated with sulfamic acid in presence of urea in homogeneous solution.

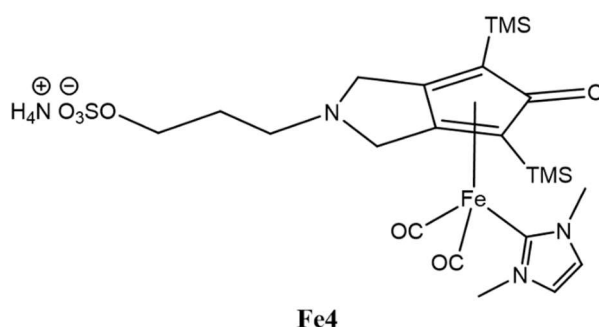


Figure 5 Fe(0) cyclopentadienone NHC complex with modifications on the alkyl backbone of the cyclopentadienone

2. Results and Discussion

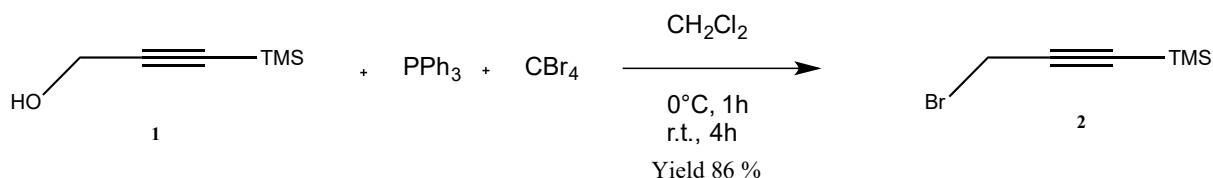
The main objective of my thesis is the insertion of a polar group in the side chain of the cyclopentadienone ligand. This insertion should guarantee a sort of solubility of the complex in aqueous environment. The possibility of acting in an aqueous environment (often in a saline phosphate buffer solution) allows us to investigate possible applications in the bioinorganic field, in particular their possible cytotoxicity. Examples of complexes with these capacities have already been reported in the literature⁴³, but to date the synthesis of iron complexes in which the ligands guarantee a tuning of both electronic, steric and solubility properties remains a challenge. In this context the research group has proposed a straightforward pathway toward the synthesis of a new family of iron(0) complexes where the combination of cyclopentadienone (CpO), N-heterocyclic carbene (NHC) and carbonyl ligands were exploited.⁴³ The following steps follow the principle adopted by the research group for the synthesis of functionalized complexes capable of acting in an aqueous environment.⁴³

Starting from the synthesis of the triscarbonyl precursor (**Fe0**), I moved on to the synthesis of the intermediate **Fe1**, where a carbonyl was replaced with the more labile acetonitrile. Then I carried out the one-pot synthesis of the complex containing the NHC ligand (**Fe2**). To achieve water solubility, a polar group is necessary so I first try the sulfonation of the precursor **Fe0** obtaining the sulfonated intermediate **Fe3**, then I achieve the synthesis of the sulfonated NHC complex **Fe4** by the insertion of the polar $-\text{OSO}_3^-$ group into the side chain of **Fe2**. The final complex **Fe4** requires further characterizations to determine the actual structure and the ability or not to dissolve, and not degrade, in an aqueous environment.

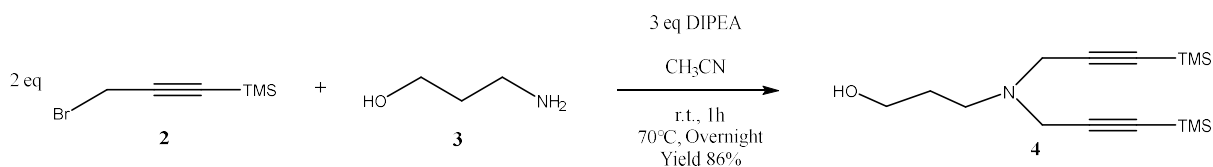
2.1 Synthesis of triscarbonyl precursor (Fe0)

The synthetic strategy of (2,4-bis(trimethylsilyl)-7-Npropan-1-ol-bicyclo[3.3.0]hepta-1,4-dien-3-one)iron triscarbonyl (**Fe0**) starts from the synthesis of (3-bromoprop-1-yn-1-yl)trimethylsilane (**2**) exploiting the Appel's reaction⁴⁴ that converts an alcohol, 3-(trimethylsilyl)prop-2-yn-1-ol (**1**), into an alkyl halide using triphenylphosphine and carbon tetrabromide in this case, yield 86% (**Scheme 7**). Subsequently the alkyl bromide (**2**) was treated with 3-aminopropan-1-ol (**3**) in presence of N,N-Diisopropylethylamine (DIPEA) as

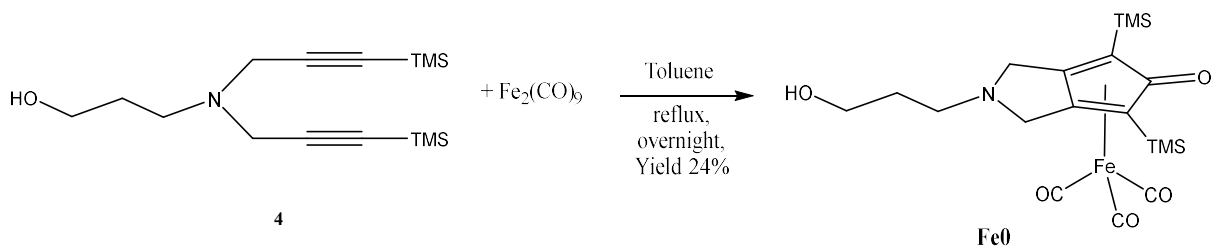
base, to achieve the alkylation of the amine, through a nucleophilic substitution as reported in literature⁴⁵, to give 3-(bis(3-(trimethylsilyl)prop-2-yn-1-yl)amino)propan-1-ol (**4**) as the product in 86% yield (**Scheme 8**). Finally, the tertiary amine in presence of di-iron nonacarbonyl leads to (2,4-bis(trimethylsilyl)-7-Npropan-1-ol-bicyclo[3.3.0]hepta-1,4-dien-3-one)iron triscarbonyl (**Fe0**), by means of cyclization reaction, yield 24% . The reaction was allowed exploiting a similar procedure reported in literature⁴³(**Scheme 9**).



Scheme 7 Synthesis of the alkyl bromide (**2**) starting from alcohol (**1**)

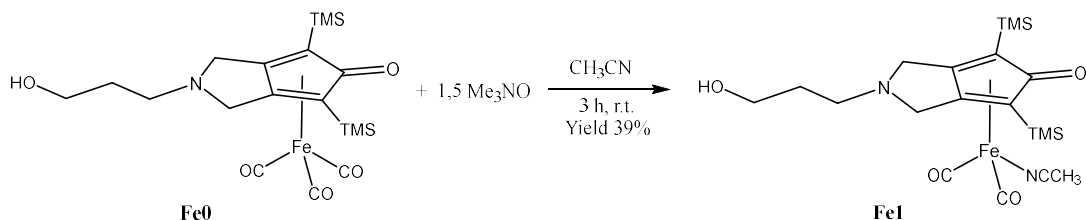


Scheme 8 Synthesis of the tertiary amine (**4**) starting from alkyl bromide (**2**) and alcohol (**3**)



Scheme 9 Synthesis of the iron triscarbonyl precursor (**Fe0**) starting from tertiary amine (**4**)

2.2 Synthesis of more labile acetonitrile dicarbonyl intermediate (**Fe1**)



By reacting (2,4-bis(trimethylsilyl)-7-Npropan-1-ol-bicyclo[3.3.0]hepta-1,4-dien-3-one)iron triscarbonyl (**Fe0**) with Me_3NO the displacement of carbonyl with the more labile acetonitrile ligand was achieved 1 equivalent of **Fe0** and 1.5 equivalent of trimethylamine-N-oxide, used

as base, were dissolved in anhydrous acetonitrile. The mixture was stirred at room temperature and protected from light for 3 hours. At the end of the reaction a yellow precipitate appeared, cause the complex is insoluble in CH₃CN. The solid was filtered and washed with diethyl ether and hexane. **Fe1** was obtained in a 39% yield. Suitable crystals for X-Ray diffraction were obtained by slow evaporation of a saturated solution of the product in EtOAc and subsequently analysed by X-ray crystallography (**Figure 7**).

The complex was analysed through NMR spectroscopy but the presence of paramagnetic high spin Fe(II) or high spin Fe(III) as possible by-products in traces, resulted in highly noisy and unresolved spectra impossible to be assigned to the product.

Anyway, the reaction was followed using IR spectroscopy until the disappearance of **Fe0** signals. Comparing **Fe0** spectrum with the one collected on pure **Fe1** (**Figure 8**), using CH₂Cl₂ as solvent, the three bands related to -CO stretching of **Fe0** on magenta respectively at 2068, 2011 and 1995 cm⁻¹, are clearly replaced by the two bands related to -CO stretching of **Fe1** on blue respectively at 2007 and 1949 cm⁻¹. The spectrum confirm the exchange of the -CO ligand, cause the related bands decrease from three to two and a shift is observed, confirming a different strength of the Fe-CO bonds and subsequently a weaker C-O bond, as confirmed by the Fe(1)-C(1) and Fe(1)-C(2) length reported on **Table 1**, after comparison with length of similar compounds with three CO ligand.. The product structure is further confirmed by the ESI-MS spectrum, in which the molecular ion is at 477 m/z and is observable the iron pattern.

Bond	Length (Å)
Fe(1)-C(1)	1.786(16)
Fe(1)-C(2)	1.786(16)
Fe(1)-N(1)	1.967(19)
Fe(1)-C(5)	2.320(20)
Fe(1)-C(6)	2.124(15)
Fe(1)-C(7)	2.123(15)
Fe(1)-C(8)	2.058(13)
Fe(1)-C(9)	2.058(13)

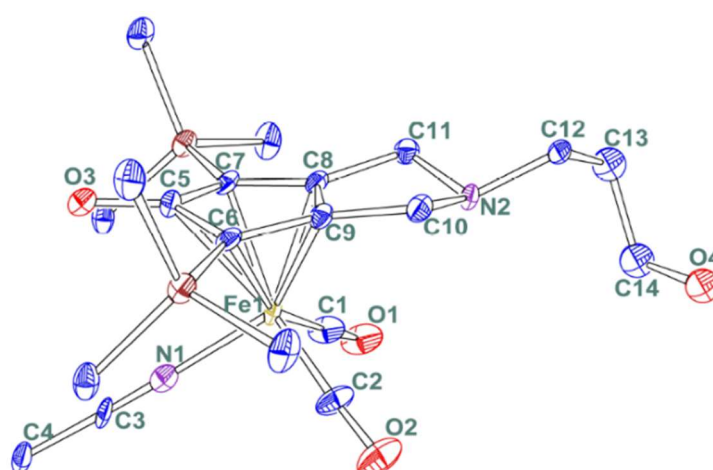


Table 6 Bonds length of **Fe1**

Figure 7 X-ray structure of the **Fe1** complex

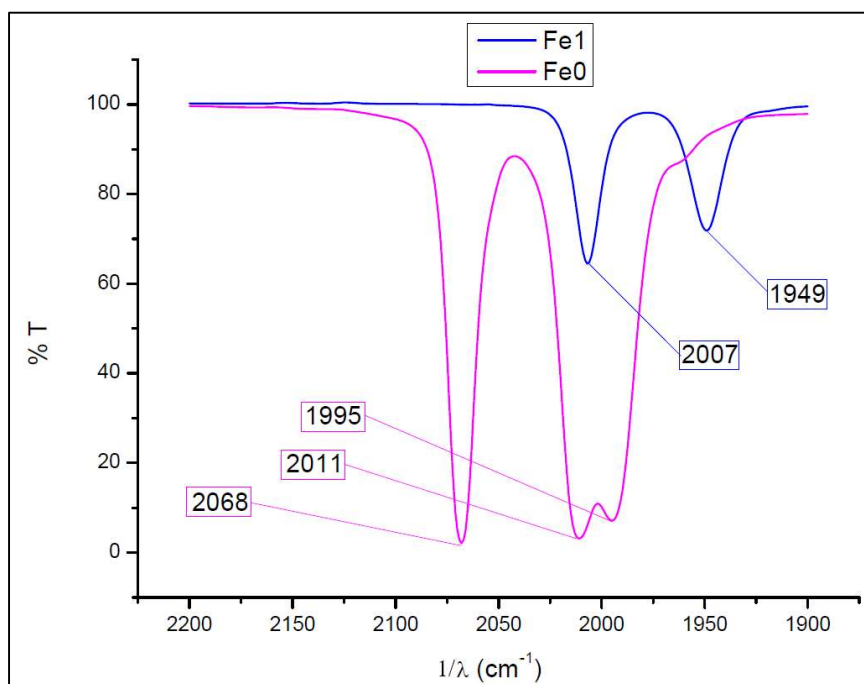
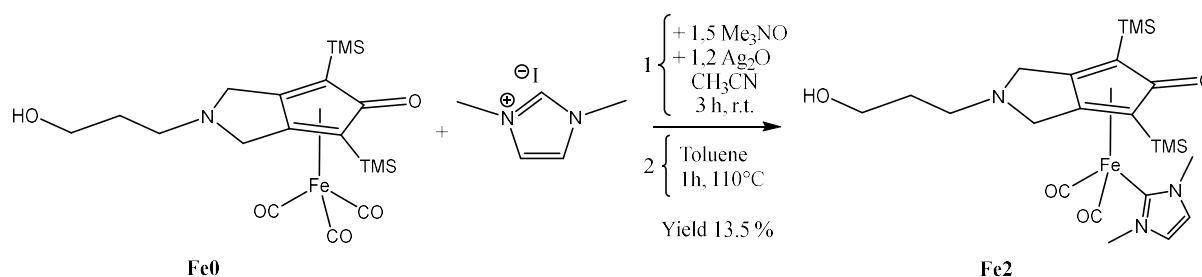


Figure 8 IR spectra of **Fe0** in magenta and **Fe1** in blue

2.2 Synthesis of NHC cyclopentadienone complex (**Fe2**)



Exploiting a silver mediated transmetalation, a one pot reaction which pass through the formation of **Fe1** as intermediate lead to the formation of the desired NHC cyclopentadienone complex **Fe2**. The reaction involves 1,3-dimethylimidazolium iodide, 1.2 equivalent of silver oxide, (2,4-bis(trimethylsilyl)-7-N-propan-1-ol-bicyclo[3.3.0]hepta-1,4-dien-3-one)iron triscarbonyl (**Fe0**) and 1.5 equivalent of trimethylamine-N-oxide as base. Adding all compounds in CH₃CN under inert atmosphere and with protection from light, the reaction was stirred for 3h at room temperature, the solvent was removed under vacuo, then the solid dissolved in toluene. The reaction mixture was stirred for 1 hour at 110°C. Upon removal of the solvent, the crude was purified to afford (2,4-bis(trimethylsilyl)-7-N-propanol-bicyclo[3.3.0]hepta-1,4-dien-3-one)iron(1,3-dimethyl-ilidene)dicarbonyl (**Fe2**) by neutral

alumina column chromatography using dichloromethane/ethyl acetate (100/0 to 0/100). Yield 13,5%. The reaction was followed using IR spectroscopy and the last spectra collected (**Figure 9**), using CH₂Cl₂ as solvent, show the disappearance of the three band related to -CO stretching of **Fe0** in black at 2068, 2011 and 1995 cm⁻¹, together with the increase frequency of the bands ascribable to **Fe2**. The shift of the wavenumber to 1988 and 1928 cm⁻¹. **Fe2** is in agreement with the structure proposed because similar to previously reported complexes with similar structure. Luckily in the latter case a clear ¹H-NMR spectrum (**Figure 10**) was obtained in CDCl₃, where are observable all the signals ascribable to **Fe2**: at 6.96 ppm the two CH of the NHC ligand, at 3.93 ppm the six proton of the two CH₃ of the NHC. Then the signals of the cyclopentadienone ligand: at 3.79 ppm the two CH₂ of the “back” ring containing the nitrogen, at 3.26, 2.98 and 1.84 ppm the signal of the three CH₂ of the alkyl backbone between the nitrogen and the hydroxyl groups (the assignation has been possible after comparison with similar complex containing the same backbone)⁴³. Other two signals are visible, the former and wider at 1.58 ppm is probably water and the latter at 1.24 ppm is an impurity or less probably the -OH group since even if it is the only proton signal absent, the integration does not match. Due to the lack of product ¹³C-NMR was hard to be registered. Further characterization will be performed in the future. The product was analysed through ESI-MS spectroscopy and the molecular ion plus sodium was observed at 554 m/z.

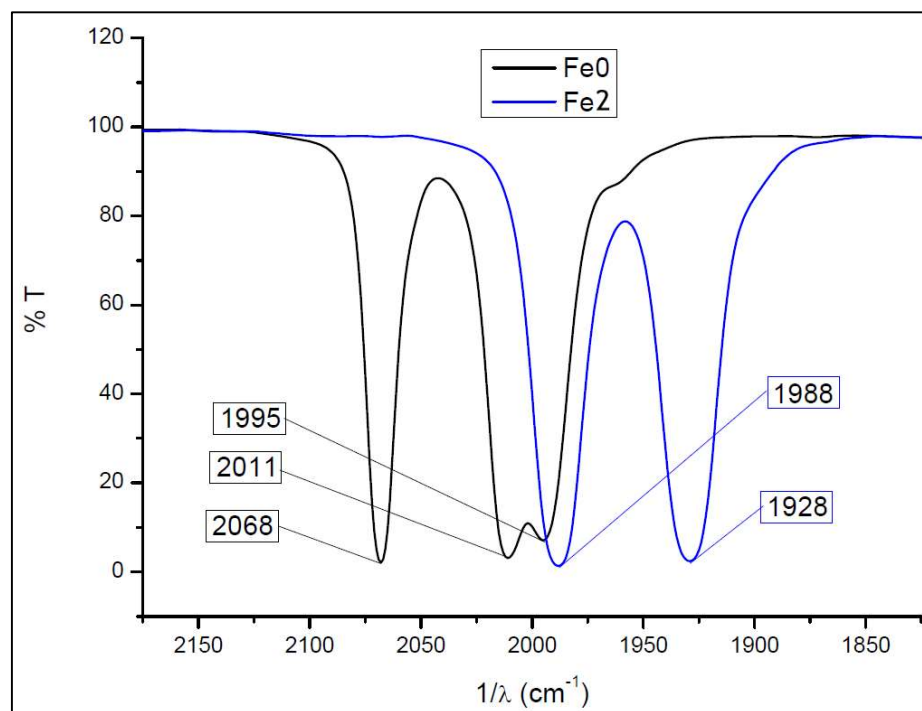


Figure 9 IR spectra of **Fe0** in black and **Fe2** in blue

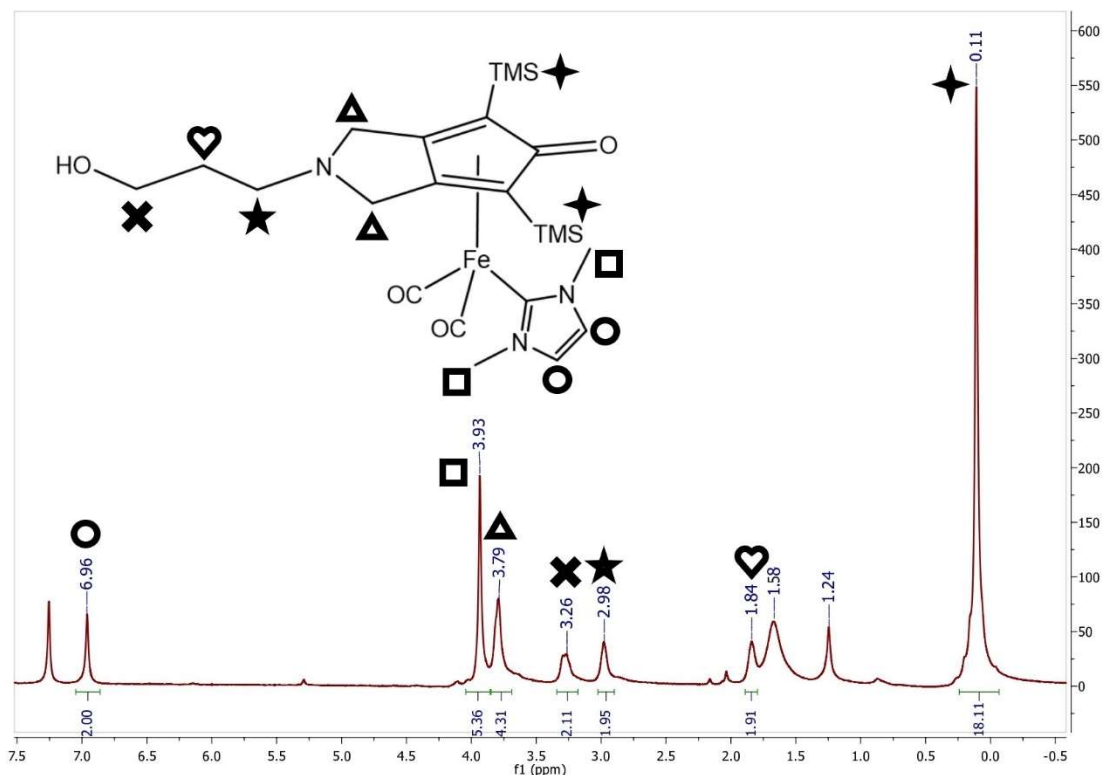
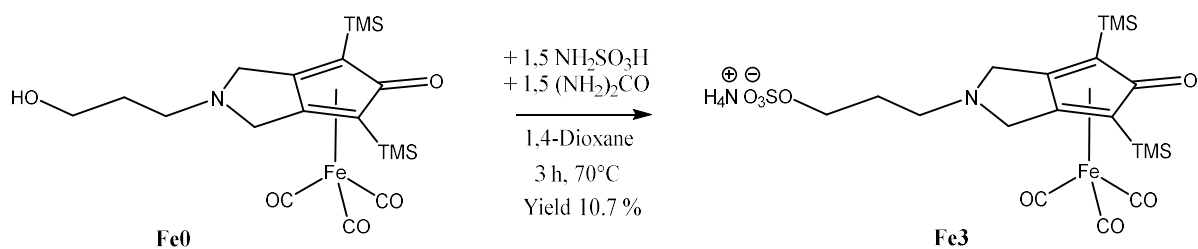


Figure 10 ¹H-NMR spectra of Fe2

2.3 Synthesis of sulfonated triscarbonyl intermediate (Fe3)

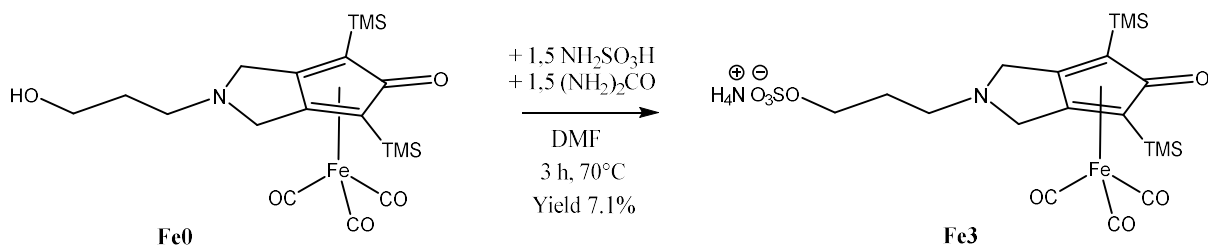
The modification of the alkyl backbone of the cyclopentadienone ligand was achieved through a sulfonation of the iron triscarbonyl precursor (**Fe0**) with sulfamic acid in 1,4-dioxane (**Procedure A**) and N,N-Dimethylformamide (**Procedure B**). The procedure used was the same found in literature⁴⁶ except for the final extraction where n-BuOH was exchanged with DCM as the organic phase.

Procedure A



(2,4-bis(trimethylsilyl)-7-N-propan-1-ol-bicyclo[3.3.0]hepta-1,4-dien-3-one)iron triscarbonyl (**Fe0**), 1.5 equivalent of urea and 1.5 equivalent of sulfamic acid, previously dried at 105°C for one night, were dissolved in 1,4-dioxane. Reaction mixture was stirred at 70°C for 3 hours. Upon removal of the solvent, the solid was dissolved in H₂O and then extracted with dichloromethane. Both the organic and aqueous phases contain the product. Yield : 10,7%

Procedure B



(2,4-bis(trimethylsilyl)-7-N-propan-1-ol-bicyclo[3.3.0]hepta-1,4-dien-3-one)iron triscarbonyl (**Fe0**), 1.5 equivalent of urea and 1.5 equivalent of sulfamic acid, previously dried at 105°C for one night, were dissolved in dimethylformamide. Reaction mixture was stirred at 70°C for 3 hours. Upon removal of the solvent, the solid was dissolved in H₂O and then extracted with dichloromethane. Both the organic and aqueous phases contain the product. Yield : 7,1%.

The complex was analysed through NMR spectroscopy but the presence of paramagnetic high spin Fe(II) or high spin Fe(III) results in high noise and an impossibility to obtain a clear spectra. The reaction was followed using IR spectroscopy and the last spectra collected (**Figure 11**), using DCM as solvent, show the three band related to -CO stretching of **Fe0** in black at 2068, 2011 and 1995 cm⁻¹, compared with red spectra of **Fe3** where the three band are shifted to different wavenumber: at 2080, 2025 and 2015 cm⁻¹. The product was characterized using ESI-MS spectroscopy, giving 542 m/z as the molecular ion registering the negative ions (NH₄⁺ as the counterion was not detectable).

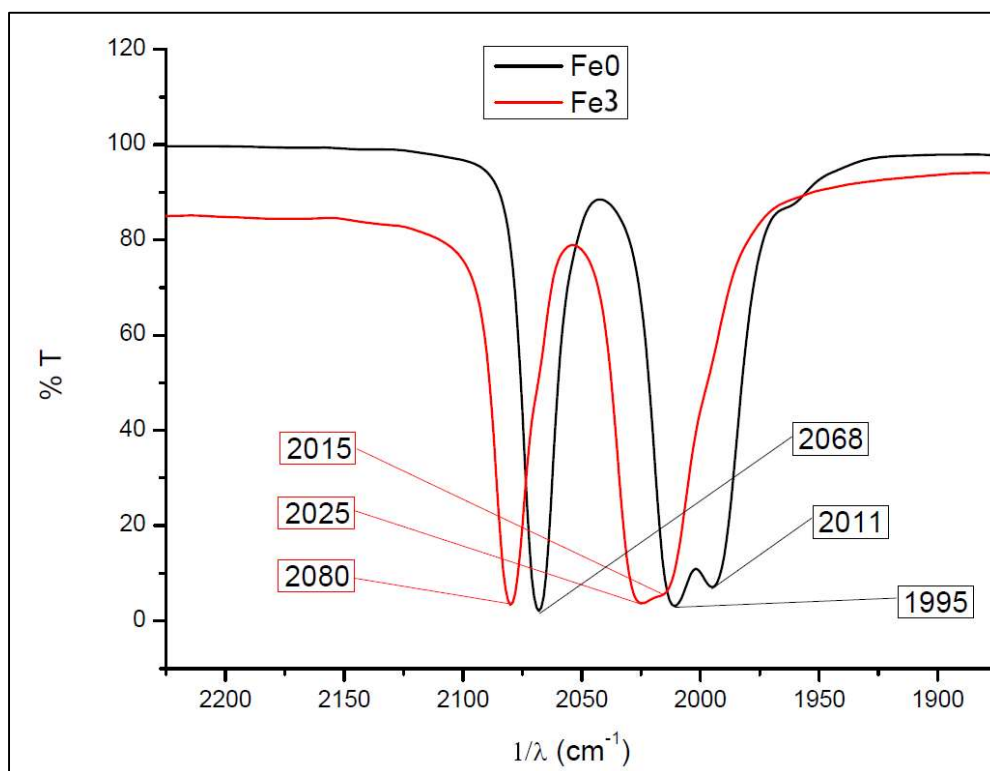
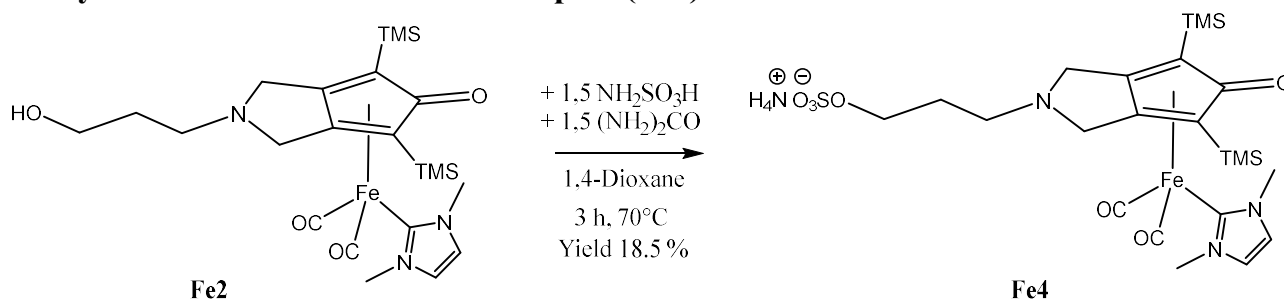


Figure 11 IR spectra of Fe0 in black and Fe3 in red

2.4 Synthesis of sulfonated NHC complex (Fe4)



The last reaction was very similar to the previous one, but the starting material this time was **Fe2** trying to observe if the presence of the NHC ligand could change the final results, 1,4-Dioxane was used as solvent cause it gave the best results in the previous reaction. (2,4-bis(trimethylsilyl)-7-N-propanol-bicyclo[3.3.0]hepta-1,4-dien-3-one)iron(1,3dimethyl-*ilidene*)dicarbonyl (**Fe2**) 1,5 equivalent of urea and 1.5 equivalent of sulfamic acid, previously dried at 105°C for one night, were dissolved in the minimum quantity of 1,4-dioxane. Reaction mixture was stirred at 70°C for 3 hours. Upon removal of the solvent, the solid was dissolved

in H₂O and then extracted with dichloromethane. Both the organic and aqueous phases contain the product. Yield : 18,5%.

The reaction was followed using IR spectroscopy and the last spectra collected (**Figure 12**), using DCM as solvent, show the two band related to -CO stretching of **Fe2** in blue and those of **Fe4** in green. Both the band have the same wavenumber: at 1988 and 1928 cm⁻¹. The absence of a band shift after ligand exchanging could be clarified following DFT calculations. Only the ESI-MS can indicate that the reaction gave **Fe4** as product, cause the molecular ion was found to be at 610 m/z (registering the negative ions) and matches with the molecular weight of **Fe4**.

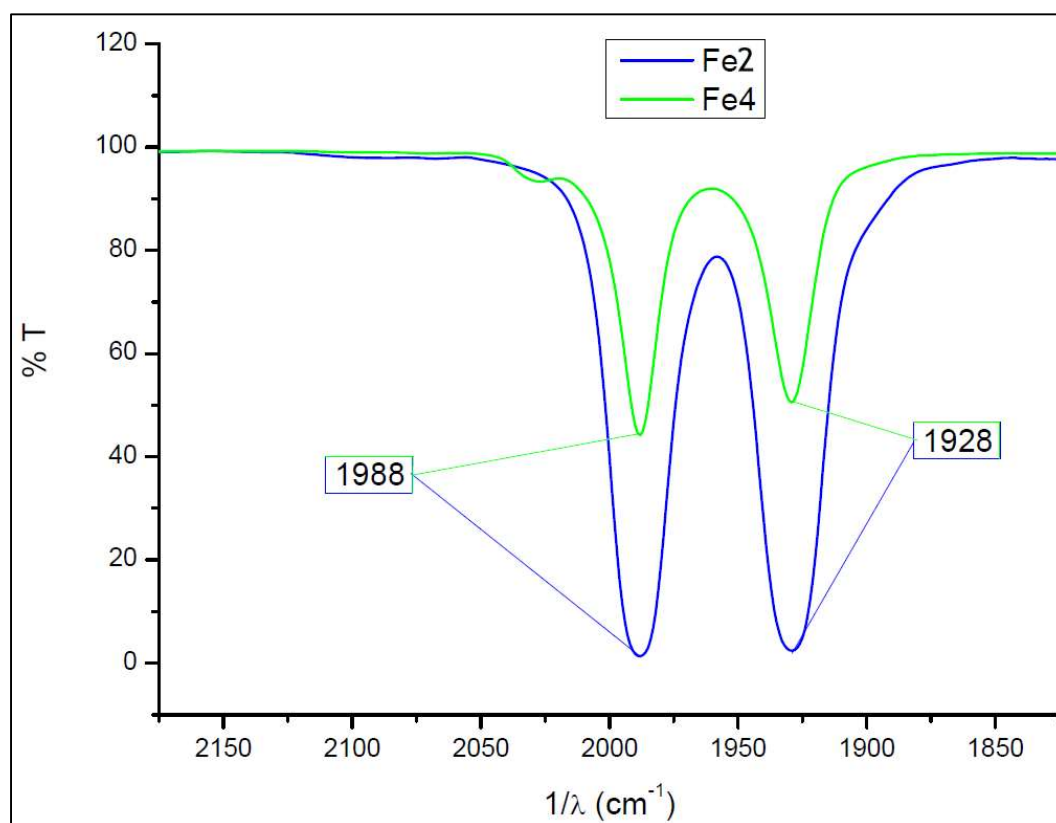


Figure 12 IR spectra of **Fe2** in blue and **Fe3** in green

3 Conclusion

The goal of the training period was to synthesize and characterize new Fe (0) complexes, containing both the cyclopentadienone ligand and NHC, responsible for the electronic and stability characteristics of the complex. In particular, were examined complexes in which the alkyl chain linked to the cyclopentadienone ring was modified, replacing the hydroxyl group with the sulphonic group, in an attempt to solubilize the complex in water, opening the possibility to numerous catalytic and biological applications.

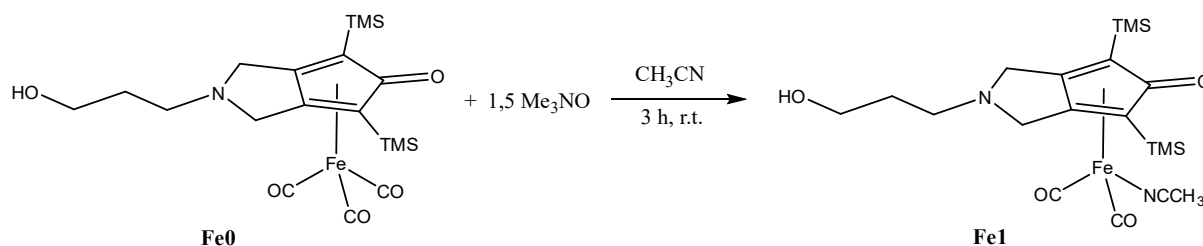
The first results of my work shows the feasibility of the synthesis which can be optimized with further tests. Future research could follow the path of this thesis achieving the synthesis of more complex with different polar group linked in different part of the complex, exploiting the easy tuning and synthesis of NHCs cyclopentadienone complexes.

4. Experimental section

General: materials and procedures

Solvents: dichloromethane (CH_2Cl_2), diethyl ether (Et_2O), N,N-dimethylformamide (DMF), acetonitrile (CH_3CN) were dried and distilled prior to use. Acetone has been degassed and stored under inert atmosphere on molecular sieves. Other solvents such as hexane, toluene, CDCl_3 (Sigma Aldrich) have been employed without further purification. Reagents: silver oxide, 1-methylimidazole, urea, sulfamic acid (Alfa Aesar) have been employed as purchased. (2,4-bis(trimethylsilyl)-7-N-propanol-bicyclo[3.3.0]hepta-1,4-dien-3-one)iron-triscarbonyl (**Fe0**) was used as synthesized from the research group, after filtration through a neutral alumina pad. The prepared derivatives were characterized by spectroscopic methods. The NMR spectra were recorded using Varian Mercury Plus VX 400 (^1H , 399.9; ^{13}C , 100.6 MHz) spectrometers at 298 K; chemical shifts were referenced internally to residual solvent peaks. Infrared spectra were recorded at 298 K on a Perkin-Elmer Spectrum 2000 FT-IR spectrophotometer. ESI-MS spectra were recorded on Waters Micromass ZQ 4000 with samples dissolved in MeOH or CH_3CN .

4.1 Synthesis of (2,4-bis(trimethylsilyl)-7-N-propan-1-ol-bicyclo[3.3.0]hepta-1,4-dien-3-one)iron acetonitrile dicarbonyl (Fe1)



In a dried 50mL Schlenk flask, (2,4-bis(trimethylsilyl)-7-Npropan-1-ol-bicyclo[3.3.0]hepta-1,4-dien-3-one)iron triscarbonyl (**Fe0**) 0.050g (0.11mmol) and trimethylamine-N-oxide 0.026g (0.35mmol) were dissolved in 10mL of anhydrous acetonitrile. Reaction mixture was stirred at room temperature and protected from light for 3 hours. A yellow precipitate appeared. The solid was filtered and washed with 10mL of diethyl ether and hexane. Crystals were obtained by slow evaporation of a saturated solution of the product in EtOAc and subsequently analyzed by X-ray crystallography (**Figure 13**). Yield: 38,9%.

The complex was analysed through NMR spectroscopy but the presence of paramagnetic Fe(II) results in high noise and an impossibility to obtain a clear spectra.

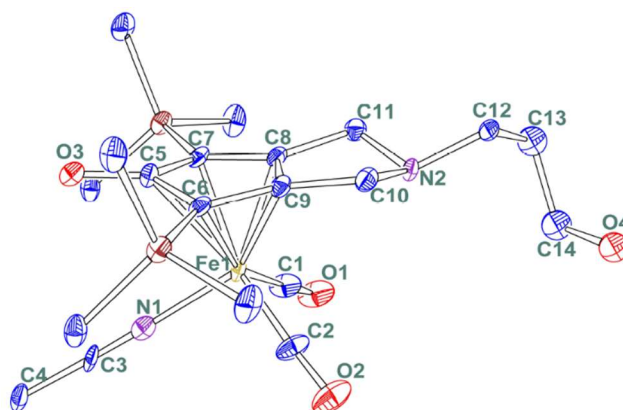


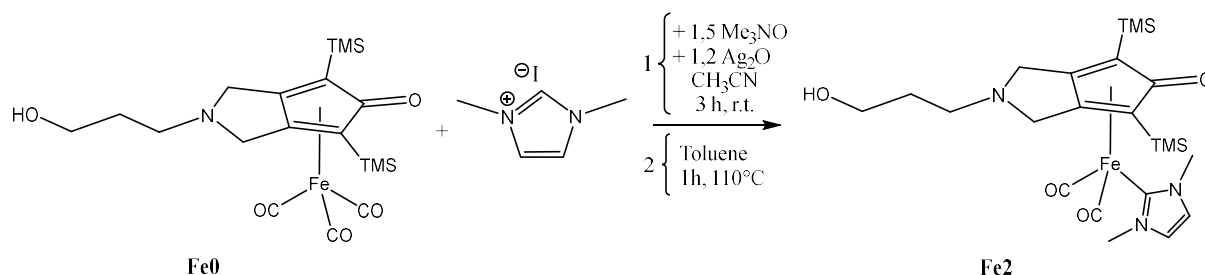
Figure 13 X-ray structure of the **Fe1** complex

Characterization

IR (CH₂Cl₂): ν 2007, 1949 cm⁻¹.

ESI-MS (m/z): 477 [M+H]⁺.

4.2 Synthesis of (2,4-bis(trimethylsilyl)-7-*N*-propan-1-ol-bicyclo[3.3.0]hepta-1,4-dien-3-one)iron(1,3-dimethyl-ilidene)dicarbonyl (Fe2)



1,3-dimethylimidazolium iodide (0.050g, 0.23mmol), silver oxide (0.065g, 0.275mmol), (2,4-bis(trimethylsilyl)-7-*N*-propan-1-ol-bicyclo[3.3.0]hepta-1,4-dien-3-one)iron tris-carbonyl (0.105g, 0.23mmol) (**Fe0**) and trimethylamine-*N*-oxide (0.026g, 0.35mmol) were reacted in CH₃CN under inert atmosphere and with protection from light. After stirring the reaction for 3h at room temperature, the solvent was removed under vacuo, then the solid dissolved in 10mL of toluene. The reaction mixture was stirred for 1 hour at 110°C. Upon removal of the solvent, the crude was purified to afford (2,4-bis(trimethylsilyl)-7-*N*-propanol-bicyclo[3.3.0]hepta-1,4-dien-3-one)iron(1,3-dimethyl-ilidene)dicarbonyl (**Fe2**) by neutral alumina column chromatography using dichloromethane/ethyl acetate (100/0 to 0/100). Yield 13,5%.

Characterization

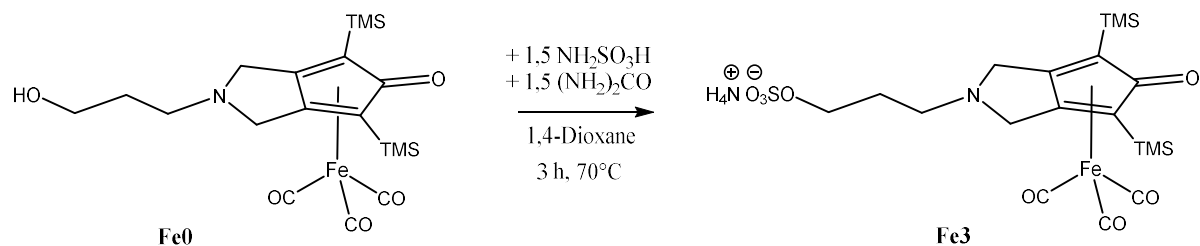
IR (CH₂Cl₂): ν 1988, 1928 cm⁻¹.

ESI-MS (*m/z*): 532 [M+H]⁺; 554 [M+Na]⁺.

¹H-NMR (400.1 MHz, CDCl₃): δ (ppm): 6.95 (s, 2H, CH_{NHC}), 3.93 (s, 6H, CH₃),

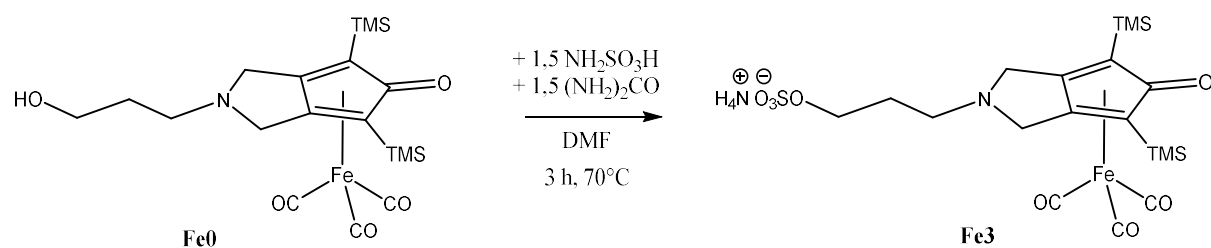
3.79 (m, 4H, CH₂ ring), 3.25 (m, 2H, CH₂ alkyl-OH), 2.96 (m, 2H, CH₂ alkyl-N), 1.84 (m, 2H, CH₂, alkyl-middle), 0.11 (s, 18H, CH₃ TMS),

4.3 Synthesis (A) of ammonium [(2,4-bis(trimethylsilyl)-7-*N*-propan-1-sulfate-bicyclo[3.3.0]hepta-1,4-dien-3-one)iron tricarbonyl] (Fe3)



In a dried 50mL Schlenk flask, (2,4-bis(trimethylsilyl)-7-*N*-propan-1-ol-bicyclo[3.3.0]hepta-1,4-dien-3-one)iron tricarbonyl (**Fe0**) 0.100g (0.22mmol), urea 0.021g (0.33mmol) and 0.045g (0.33mmol) sulfamic acid, previously dried at 105°C for one night. The solids were dissolved in 5mL of 1,4-dioxane. Reaction mixture was stirred at 70°C for 3 hours. Upon removal of the solvent, the solid was dissolved in 10mL of H₂O and then extracted with 3x10mL of dichloromethane. Both the organic and aqueous phases contain the product. Yield : 10,7%

4.4 Synthesis (B) of ammonium [(2,4-bis(trimethylsilyl)-7-*N*-propan-1-sulfate-bicyclo[3.3.0]hepta-1,4-dien-3-one)iron tricarbonyl] (Fe3)



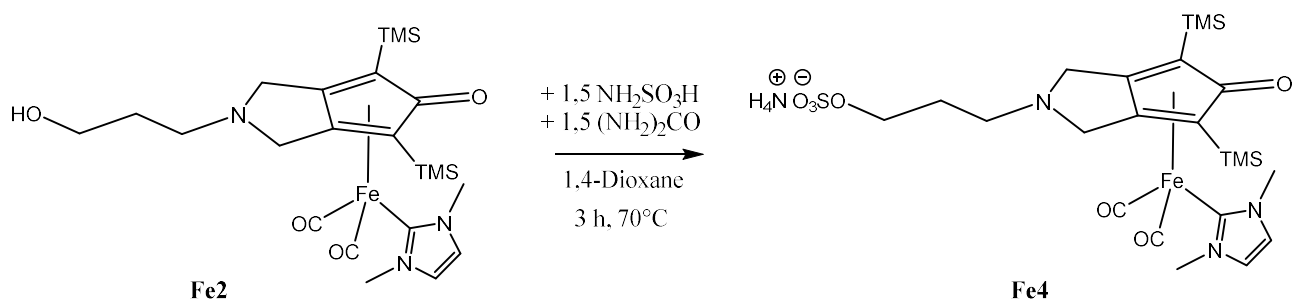
In a dried 50mL Schlenk flask, (2,4-bis(trimethylsilyl)-7-*N*-propan-1-ol-bicyclo[3.3.0]hepta-1,4-dien-3-one)iron tricarbonyl (**Fe0**) 0.100g (0.22mmol), urea 0.021g (0.33mmol) and 0.045g (0.33mmol) sulfamic acid, previously dried at 105°C for one night. The solids were dissolved in 5mL of dimethylformamide. Reaction mixture was stirred at 70°C for 3 hours. Upon removal of the solvent, the solid was dissolved in 10mL of H₂O and then extracted with 3x10mL of dichloromethane. Both the organic and aqueous phases contain the product. Yield : 7,1%. The complex was analysed through NMR spectroscopy but the presence of paramagnetic Fe(II) results in high noise and an impossibility to obtain a clear spectra.

Characterization

IR (CH₂Cl₂): ν 2080, 2025, 2015 cm⁻¹.

ESI-MS (m/z): 542 [M]⁻.

4.5 Synthesis of ammonium [(2,4-bis(trimethylsilyl)-7-N-propan sulfato-bicyclo[3.3.0]hepta-1,4-dien-3-one)iron(1,3-dimethyl-ilidene) dicarbonyl] (Fe3)



In a dried 50mL Schlenk flask, (2,4-bis(trimethylsilyl)-7-N-propanol-bicyclo[3.3.0]hepta-1,4-dien-3-one)iron(1,3-dimethyl-ilidene)dicarbonyl (**Fe2**) 0.100g (0.19mmol), urea 0.017g (0.29mmol) and 0.028g (0.29mmol) sulfamic acid, previously dried at 105°C for one night. The solids were dissolved in 5mL of 1,4-dioxane. Reaction mixture was stirred at 70°C for 3 hours. Upon removal of the solvent, the solid was dissolved in 10mL of H₂O and then extracted with 3x10mL of dichloromethane. Both the organic and aqueous phases contain the product. Yield : 18,5%

Characterization

IR (CH₂Cl₂): ν 1988, 1928 cm⁻¹.

ESI-MS (m/z): 610 [M]⁻.

5 Reference

Chapter I

1. Dahl, S.; Chorkendorff, I. Solar-Fuel Generation Towards Practical implementation. *Nat. Mater.* **2012**, 11 (2), 100-101.
2. Gang J.; Liang. J.; Sumathy, K. Review on Dye-Sensitized Solar Cells (DSSCs): Fundamental Concepts and Novel Materials, *Renew. Sustain. Energy Rev.* **2012**, 16 (8), 5848-5850.
3. Kabir, E.; Kurnar. P.; Kumar. S; Adelodun, A. A.; Kim, K. H, Solar Energy: Potential and Future Prospects. *Renew. Sustain. Energy Rev.* **2018**, 82 (October 2017). 894-900.
4. imamzai. M.J Aghael, M.; Thayoob, Y. H. A Review on Comparison between Traditional Silicon Solar Cells and Thin- Film CdTe Solar Cells. *Proc. Natl. Grad. Conf.* **2011**, 2012 (November 2012). 8-10.
5. Gratzel, M. Dye-Sensitized Solar Cells. *J. Photochem. Photobiol. C Photochem. Rev* **2003**, 4 (2), 145-153.
6. Suzuka, M.; Hayashi, N.; Sekiguchi, T.; Sumioka, K.; Takata, M.; Hayo, N.; ikeda, H.; Oyaizu, K.; Nishide, H. A Quasi-Solid State DSSC with 10 10% Efficiency through Molecular Design of the Charge-Separation and -Transport. *Sci. Rep.* **2016**, 6 (June), 1-7.
7. Sharma, K.; Sharma, V.; Sharma. S. S. Dye-Sensitized Solar Cells : Fundamentals and Current Status. **2018**, 6.
8. Oin. P.; Zhu, H. J.; Edvinsson, T.; Boschloo, G.; Hagfeldt, A.; .Sun. L. C., Design of an Organic Chromophore for P-Type Dye-Sensitized Solar Cells (Vol 130, Pg 8570, 2008) *J. Am. Chem. Soc.* **2008**, 130 (51), 17629.
9. Kakiage, K.; Aoyama, Y.; Yano, T.; Oya, K.; Fujisawa, J. I.; Hanaya, M. Highly-Efficient Dye-Sensitized Solar Cells with Collaborative Sensitization by Silil-Anchor and Carboxi-Anchor Dyes. *Chem. Commun.*, 2015, 51 (88) 15894-15897.
10. Pham, T. T. T.; Saha, S. K.; Provost, D.; Farré, Y.; Raissi. M.; Pellegrin. Y.; Blart. E.; Vedraïne, S.; Ratier, B.; Aldakov. D.; et al Toward efficient Solid-State p-Type Dye-Sensitized Solar Cells: The Dye Matters. *J Phys. Chem. C* **2017**, 121 (1), 129-139.
11. Hamilton, D. G.; Feeder, N.; Prodi. L ; Teat. S. J.; Clegg. W.; Sanders. J. K. M. M., Blart, E., Spectus, C. O. N.; Sreevatsa; Williams, R; el al. introduction to Electron Transfer, *J. Am. Chem. Soc.*, **2008**, 41 (11), 8570-8571.
12. Ye, M.; Wen, X.; Wang, M ; iocozzia, J.; Zhang, N.; Un, C.; Lin, 2. Recent Advances in Dye-Sensitized Solar Cells: From Photoanodes, Sensitizers and Electrolytes to Counter Electrodes. *Mater Today*, **2015**, 18 (3), 155-162.
13. Perera, i. R.; Daeneke, T., Makuta. S.; Yu, Z.; Tachibana, Y., Mishra, A ; Bauerle, P.; Ohlin, C. A.; Bach. U.; Spiccia. L. Application of the Tris(Acetylacetonato)iron(III)/(II) Redox Couple in p-Type Dye-Sensitized Solar Cells. *Angew. Chemie - int. Ed.* **2015**, 54 (12), 3758-3762.
14. Vossler. A.; Gualdl. F.; Dollet. A., Ares, R., Aimez, Y. Approaching the Shockley-Queisser Limit: General Assessment of the Main Limiting Mechanisms in Photovoltaic Cells. *J. Appl. Phys.* **2015**, 117 (1).
15. Vos, A. De. Detailed balance Limit of the Efficiency of Tandem Solar Cells. *J. Phys. D. Appl. Phys.*, **1980**, 13 (5) 839-846.
16. Crablee. G. W.; Lewis, N. S. Solar Energy Conversion. *Plant, Cell Environ.* **2007**, No. March, 37.
17. Huang, Z.; Natu, G.; Ji, Z.; Hasin, P.; Wu, Y. P-Type Dye-Sensitized NiO Solar Cells: A Study by Electrochemical impedance Spectroscopy. *J Phys. Chem. C* **2011**. 115 (50), 25109-25114.

18. Powar, S.; Daeneke, T., Ma, M. T.; Fu, D.; Duffy, N. W.; GCTz. G.; Weldelener, M.; Mishra. A ; BAuerle. P.; Spiccla. L. *Angewandte Solar Cells Highly Efficient P-Type Dye-Sensitized Solar Cells Based on Tris (1, 2-Diaminoethane) Cobalt (II)/(III) Electrolytes.* **2013**, 602-605.
19. Nartestad, A.; Mozer, A.J.; Fischer, M. K. R.; Cheng, Y. B ; Mishra. A.; Buerle, P., Bach, U. *Highly Efficient Photocathodes for Dye-Sensitized Tandem Solar Cells.* *Not. Mater* **2010**, 9 (1), 31-35.
20. Hush, N. S.e, 64 (1985) 135-157. **2006**, 64 (1985). 135-157.
- 21 Marcus, R.A *Electron Transfer Reactions in Chemistry. Theory and Experiment.* *Rev. Mod. Phys.* **1999**. 65 (3), 1203-1215.
22. Merker, S.; Krautscheld, H.; Zahn, S. *Can a Temporary Bond between Dye and Redox Mediator Increase the Efficiency of P-Type Dye-Sensitized Solar Cells?* *J. Mol. Model* **2018**, 24 (11). 5-8.
23. Parlane, F. G, L; Mustoe, C.; Kellett. C. W.; Simon, S. j.: Swords, W. B.; Meyer, G. J.; Kennepahl. P.; Berlinguette. C. P. *Spectroscopic Detection of Halogen Bonding Resolves Dye Regeneration in the Dye-Sensitized Solar Cell.*, *Vat. Commun.* **2017**, 8 (1), 1-8.
24. Hunter. C. A.; Sanders, J. K. M. *The Nature of Pi.-Pi. interactions.* *J. Am. Chem Soc.* **2005**, 111 (14), 5525-5534.
25. Martinez. C. R.; Iversan, B. L. *Rethinking the Term “PI-Stacking.”* *Chem Sci.* **2012**, No 7, 2191-2201.
26. Qin. P ; Zhu, H.; Edvinsson, T ; Boschico, G.; Hagfeldt, A.; Sun. L. *Design of an Organic Chromophore for P-Type Dye-Sensitized Solar Cells.* *Am. Chem. Soc.* **2008**, 130 (27), 5570-5571.
27. Wood. C. J.; Mc.Gregor, C. A.: Gibson, E. *A Does Iodine or Thiocyanate Play a Role in P-Type Dye-Sensitized Solar Cells?* *Owen ElectrtoChem* **2015**, 3 (11), 1827-1836.
28. Odobel, F.; le Pleux. L ; Pellegrin, Y.; Blart. E. *New Photovoltaic Devices Based on the Sensitization of P-Type Semiconductors :* *Acc. Chem. Res.* **2010**, 43 (8). 1063-1071.
29. Boschloo. G.; Halfgeldt, A.; Spectus, C. O. N. *Characteristics of the Iodide /Triiodide Redox Mediator in Dye-Sensitized Solar Cells.* *Acc. Chem. Res.* **2009**, 42 (11), 1819-1826.
30. Odobel. F.; Pellegrin, Y.; Gibson, E. A., Hagfeldt. A.; Smelgh, A. L.; Hammarstresm, L. *Recent Advances and Future Directions to Optimize the Performances of P-Type Dye-Sensitized Solar Cells.* *Coord. Chem. Rev.* **2012**, 256 (21-2.2), 2414-2423.
31. Ashton. P. R.; Baxter, I.; Fyfe, M. C. T.; Raymo, F. M.; Spencer. N.; Stoddart. J. F.; White, A. J. P.; Wllllams, D. J. *Rotaxane or Pseudorotaxane? That is the Question!* *J. Am Chem. Soc* **1998**, 120 (1D0). 2297-2307.
32. Credi, A.; Maniati, M.; Balzarll. v.; Langford, S. J.; Rayrno. F. Mj Stocidart.J F. *Simple Molecular-Level Machines. interchange between Different Threads in Pseudorotaxanes.* *New J. Chem.* **1998**, 22 1101, 1061-1065.
33. Asakawa, M. *Prototype of an Optically Responsive Molecular Switch Based on Pseudorotaxane.* *Angew. Chemie (International Ed. English)* **1996**, 35 (9), 976-978.
34. Bouwenr, T; Mathew, S., Reek, J. N. H. *P-Type Dye-Sensitized Solar Cells based on Pseudorotaxane Mediated Charge-Transfer.* *Faraday Discuss.* **2019**. 213, (1).
35. Li, N.; Gibson, E. A.; Qin, P.; Haschloo, G.: Garlov, M.l Hagfeldt, A.; Sun. L. *Double-Layered NiO Photocathodes for p-Type DSSCs with Record IPCE,* *Adv. Mater.* **2010**, 22 (15), 1759-1762.
36. Bhosale. S. V.; Janl, C. H.; Langford, S. J. *Chemistry of Naphthalene Diimides.* *Chem. Soc. Rev* **2008**, 97 (2). 331-342.

37. Hansen, J. G.; Feeder, N.; Hamilton, D. G.; Gunter, M. J.; Becher, J.; Sanders, J. K. M. Macrocyclization and Molecular interlocking via Mitsunobu Alkylation: Highlighting the Role of C-H...O interactions in Templating. *Org. Lett.* **2000**, 2 (4), 449-452.

38. He, J.; Lindström, H.; Hagfeldt, A.; Lindqvist, S. -E. Dye-Sensitized Nanostructured p-Type Nickel Oxide Film as a Photocathode for a Solar Cell. *J. Phys. Chem. S.* **1999**, 103 (42), 8940-8943.

Chapter II

1. C. K. Jørgensen; *Coord. Chem. Rev.*, **1966**, 1, 164.
2. P. J. Chirik; K. Wieghardt; *Science*, **2010**, 327, 794.
3. V. Lyaskovskyy; B. d. Bruin; *ACS Catal.*, **2012**, 2, 270.
4. L. Que; W. B. N. Tolman; *Nature*, **2008**, 455, 333.
5. B. L. Small; M. Brookhart; *J. Am. Chem. Soc.*, **1998**, 120, 7143.
6. K. T. Sylvester; P. J. Chirik; *J. Am. Chem. Soc.*, 2009, 131, 8772.
7. G. J. P. B. et. al.; *Chem. Commun.*, **1998**, 849, 1998.
8. B. L. Conley; M. K. Pennington-Boggio; E. Boz; T. J. Williams; *Chem. rev.*, **2010**, 110, 2294.
9. H. J. Knölker; E. Baum; H. Goesmann; R. Klaus; *Angew. Chem. Int. Ed.*, 1999, 38, 2064.
10. G. N. Schrauzer; *J. Am. Chem. Soc.*, 1959, 81, 5307.
11. H.-J. Knölker; E. Baum; H. Goesmann; R. Klaus; *Angew. Chem. Int. Ed.*, 1999, 38, 2064.
12. C. P. Casey; H. Guan; *J. Am. Chem. Soc.*, **2007**, 129, 5816.
13. C. P. Casey; H. Guan; *J. Am. Chem. Soc.*, **2008**, 131, 2499.
14. A. Quintard; J. Rodriguez; *Angew. Chem. Int. Ed.*, **2014**, 53, 4044.
15. T.-T. Thai; D. S. Mörel; A. Poater; S. Gaillard; J.-L. Renaud; *Chem. Eur. J.*, **2015**, 21, 7066.
16. D. S. Mérel; M. Elie; J.-F. Lohier; S. Gaillard; J.-L. Renaud; *Chem. Cat. Chem.*, **2013**, 5, 2939.
17. S. Moulin; H. Dentel; A. Pagnoux-Ozherelyeva; S. Gaillard; A. Poater; L. Cavallo; J.-F. Lohier; J.-L. Renaud; *Chem. Eur. J.*, **2013**, 19, 17881.
18. A. Berkessel; S. Reichau; A. v. d. Höh; N. Leconte; J.-M. Neudörfl; *Organometallics*, **2011**, 30, 3880.
19. S. Díez-González; S. Nolan; *Coordination Chemistry Reviews*, **2007**, 251, 874.
20. S. T. Liddle; I. S. Edworthy; P. L. Arnold; *Chem. Soc. Rev.*, **2007**, 36, 1732.
21. E. Fischer; A. Maasböl; *Angew. Chem. Int. Ed.*, **1964**, 3, 580.
22. R. Schrock; *J. Am. Chem. Soc.*, **1974**, 96, 6796.
23. H. Wanzlick; H.-J. Schönherr; *Angew. Chem. Int. Ed.*, **1968**, 7, 141.
24. K. Öfele; a) *J. Organomet. Chem.*, **1968**, 12, P42 b) *Angew. Chem. Int. Ed.*, **1970**, 9, 739 c) *J. Organomet. Chem.*, **1970**, 22, C9.
25. A. A. III; R. Harlow; M. Kline; *J. Am. Chem. Soc.*, **1991**, 113, 361.
26. F. E. Hahn; M. C. Jahnke; *Angew. Chem. Int. Ed.*, **2008**, 47, 3122.
27. M. N. Hopkinson; C. Richter; M. Schedler; F. Glorius; *Science*, **2014**, 310, 485.
28. M. K. Denk; J. M. Rodezno; S. Gupta; A. J. Lough; *J. Organomet. Chem.*, **2001**, 242, 617.
29. L. Perrin; E. Clot; O. Eisenstein; J. Loch; R. Crabtree; *Inorg. chem.*, **2001**, 40, 5806.
30. C. M. Crudden; D. P. Allen; *Coord. Chem. Rev.*, **2004**, 248, 2247.

31. H. M. J. Wang; I. J. B. Lin; *Organometallics*, **1998**, *17*, 97.
32. H. Jacobsena; A. Correab; A. Poaterb; C. Costabile; L. Cavallo; *Coordination Chemistry Reviews*, **2009**, *253*, 867.
33. F. E. Hahn; L. Wittenbecher; D. L. Van; R. Fröhlich; *Angew. Chem. Int. Ed.*, **2000**, *39*, 541.
34. N. Metzler-Nolte, Z. Guo, *Dalton. Trans.* **2016**, *45*, 12965.
35. Z. Guo, P. J. Sadler, *Angew. Chem. Int. Ed.* **1999**, *38*, 1512.
36. E. Alessio, Z. Guo, *Eur. J. Inorg. Chem.* **2017**, 1539.
37. P. C. Bruijninx, P. J. Sadler, *Curr. Opin. Chem. Biol.* **2008**, *12*, 197.
38. M. Arredondo, M. T. Núñez, *Mol. Aspects Med.* **2005**, *26*, 313.
39. G. Patra, *Nat. Rev. Chem.* **2017**, *1*, 0066.
40. C. Lu, J. M. Heldt, M. Guille-Collignon, F. Lemaître, G. Jaouen, A. Vessières, C. Amatore, *ChemMedChem* **2014**, *9*, 1286.
41. H. Z. S. Lee, O. Buriez, F. Chau, E. Labbé, R. Ganguly, C. Amatore, G. Jaouen, A. Vessières, W. K. Leong, S. Top, *Eur. J. Inorg. Chem.* **2015**, *2015*, 4217.
42. A. Cingolani, C. Cesari, S. Zacchini, V. Zanotti, M. C. Cassani, R. Mazzoni, *Dalton. Trans.* **2015**, *44*, 19063.
43. A. Cingolani, V. Zanotti, S. Zacchini, M. Massi, P. V. Simpson, N. M. Desai, I. Casari, M. Falasca, L. Rigamonti and R. Mazzoni, *Appl. Organomet. Chem.*, **2019**, *33*, e4779.
44. R. Appel; *Angew. Chem., Int. Ed. Engl.*; **1975**, *14*, 801–811.
45. M.B. Smith; *March's Advanced Organic Chemistry: Reactions, Mechanisms, and Structure, 8th Edition*, **2019**, New York: Wiley.
46. Levdanskii, V.A., Levdanskii, A.V. & Kuznetsov, B.N. Sulfonation of Betulinic Acid by Sulfamic Acid. *Chem Nat Compd*, **2015**, *51*, 894–896.